Materials Science & Engineering C 128 (2021) 112345

Contents lists available at ScienceDirect

Materials Science & Engineering C

journal homepage: www.elsevier.com/locate/msec

Sulforaphane-loaded hyaluronic acid-poloxamer hybrid hydrogel enhances cartilage protection in osteoarthritis models

Monica Helena Monteiro do Nascimento [a,b], Felipe Nogueira Ambrosio [c], Débora Carajiliascov Ferraraz [c], Hermann Windisch-Neto [c], Samyr Machado Querobino [a], Michelle Nascimento-Sales [a], Carlos Alberto-Silva [a], Marcelo Augusto Christoffolete [a], Margareth K.K.D. Franco [d], Ben Kent [e,f], Fabiano Yokaichiya [g,h], Christiane Bertachini Lombello [c], Daniele Ribeiro de Araujo [a,b,*]

[a] Human and Natural Sciences Center, ABC Federal University, Santo André, SP, Brazil
[b] Drugs and Bioactives Delivery Systems Research Group – SISLIBIO, Federal University of ABC. Santo André, SP, Brazil
[c] Engineering, Modelling and Applied Social Sciences Center, ABC Federal University, Santo André, SP, Brazil
[d] Instituto de Pesquisas Energéticas e Nucleares-IPEN, São Paulo, SP, Brazil
[e] Institute for Soft Matter and Functional Materials, Helmholtz-Zentrum Berlin für Materialien, Berlin, Germany
[f] School of Chemistry, University of New South Wales, Kensington, Australia
[g] Department Quantum Phenomena in Novel Materials Helmholtz-Zentrum Berlin für Materialien, Berlin, Germany
[h] Department of Physics, Federal University of Parana, Curitiba, Paraná, Brazil

ARTICLE INFO

Keywords:
Sulforaphane
Poloxamer
Hyaluronic acid
Hydrogels
Osteoarthritis

ABSTRACT

Sulforaphane (SFN) is an isothiocyanate with anti-arthritic and immuno-regulatory activities, supported by the downregulation of NF-κB pathway, reduction on metalloproteinases expression and prevention of cytokine-induced cartilage degeneration implicated in OA progression. SFN promising pharmacological effects associated to its possible use, by intra-articular route and directly in contact to the site of action, highlight SFN as promising candidate for the development of drug-delivery systems. The association of poloxamers (PL) and hyaluronic acid (HA) supports the development of osteotrophic and chondroprotective pharmaceutical formulations. This study aims to develop PL-HA hybrid hydrogels as delivery systems for SFN intra-articular release and evaluate their biocompatibility and efficacy for osteoarthritis treatment. All formulations showed viscoelastic behavior and cubic phase organization. SFN incorporation and drug loading showed a concentration-dependent behavior following HA addition. Drug release profiles were influenced by both diffusion and relaxation of polymeric chains mechanisms. The PL407-PL338-HA-SFN hydrogel did not evoke pronounced cytotoxic effects on either osteoblast or chondrosarcoma cell lines. *In vitro/ex vivo* pharmacological evaluation interfered with an elevated activation of NF-κB and COX-2, increased the type II collagen expression, and inhibited proteoglycan depletion. These results highlight the biocompatibility and the pharmacological efficacy of PL-HA hybrid hydrogels as delivery systems for SFN intra-articular release for OA treatment.

1. Introduction

Osteoarthritis (OA) is a chronic and degenerative joint disease, leading to morphological, biochemical, and biomechanical alterations resulting in cartilage degeneration [1]. In the pathophysiology of OA, chondrocytes move to a degradative phenotype where NF-κB transcription factors lead to the secretion of many degradation enzymes, including Metalloproteinases (MMPs) and the Protein Disintegrin and Metalloproteinase with Thrombospondin Motives (ADAMTS), leading to articular cartilage degradation [2]. In addition, chondrocytes express a large amount of NF-κB-mediated catabolic cytokines such as interleucine 1β (IL-1β), which increase the production of MMPs, decrease collagen synthesis and proteoglycan and act in a positive feedback loop to increase NF-κB activation [3]. Finally, NF-κB molecules increase joint

* Corresponding author at: Drug and Bioactives Delivery Systems Research Group-SISLIBIO. Human and Natural Sciences Center, ABC Federal University, Santo André, SP, Brazil. Av. dos Estados 5001, Bloco A, Torre 3, Lab 503-3, Bairro Bangu, Santo André, SP CEP 090210-580, Brazil.
E-mail address: daniele.araujo@ufabc.edu.br (D.R. de Araujo).

https://doi.org/10.1016/j.msec.2021.112345
Received 27 April 2021; Received in revised form 3 July 2021; Accepted 26 July 2021
Available online 31 July 2021

induction of nitric oxide (NO), cyclooxygenase 2 (COX-2), nitric oxide synthase (iNOS) and prostaglandin E2 (PGE2), which promote the synthesis of catabolic factors, inflammation of cartilage and chondrocyte apoptosis [4–7,94].

OA pharmacotherapy refers to the symptomatic relief of OA using corticosteroid injections, and the oral administration of non-steroidal anti-inflammatory or antirheumatic drugs [2] and is frequently associated with side effects. Since intra-articular (IA) injection is one of the most commonly therapies to alleviate symptoms and prevent the progression of OA, its purpose is to maintain the drug at the site of action and to avoid fast drug uptake, thus minimizing the systemic toxic effects [8,9]. Thus, novel polymeric self-assembled hydrogels are interesting strategies for promoting enhanced therapeutic efficacy using biocompatible and osteotrophic biomaterial formulations.

As drug model in this study, we have selected sulforaphane (SFN), which is an isothiocyanate compound, extracted from cruciferous vegetables of the *Brassicaceae* family (such as broccoli), with potent anti-inflammatory and anti-carcinogenic properties. SFN can repress the expression of the metalloproteinases implicated in OA, downregulates NF-κB pathway, inhibits the prostaglandin E2 production in chondrocytes, and prevent cytokine-induced cartilage degeneration [4–7,95]. The pharmacological effects highlight SFN as an effective drug for OA treatment and a promising candidate for the development of drug-delivery systems [9].

In this sense, hyaluronic acid (HA) is of great interest as a scaffold due to its biodegradability, biocompatibility, high potential drug loading, targeting ability (selective interactions with CD44 receptors, for example), and anti-inflammatory properties [10–12]. As a component of the synovial fluid, HA acts as a lubricant and a shock absorber during joint movements, but its concentration and molecular weight are reduced in joints affected by OA. Although IA administration of HA is described as a tool to restore the synovial fluid viscosity and protect the cartilage against erosion [13,14] this therapy requires multiple injections and is associated with being a painful procedure and with risk of infection [15,16].

In addition, poloxamers (PL), copolymers composed of basic units of polyethylene oxide (PEO) and polypropylene oxide (PPO), have been investigated as drug-delivery systems and have shown promising results in terms of the improvement of biopharmaceutics properties [17,18,91]. PL can form hydrogels in response to physiological temperature and concentration, due to their sol-gel transition properties, which favor their parenteral administration and the ability to modulate drug release rates for a long period of time [19,89,90]. In fact, studies reported that PL/HA blends formulations had improved rheological properties due to interactions of HA with PL-micelles, [20,21]. *In vitro* release assays showed that PL/AH (especially PL 407) was able to control the release of acyclovir [20,21], growth hormone and ciprofloxacin [22], for different purposes such as ophthalmic route and vaginal mucosa application. However, none of those formulations were designed for OA treatment, neither used PL-based binary systems (such as PL407 and PL338, which their nomenclature defined by the three numbers referred to the approximate polyoxypropylene core molecular mass, with the first two digits multiplied by 100, and the polyoxyethylene content multiplied by 10, expressed as percentage) with different hydrophilic-lipophilic balances (HLB values of 22 and 28 for PL407 and PL338, respectively) and PEO:PPO units ratio (PL407 ~ 1:3 and PL338 ~ 1:5). Then, those hybrid hydrogels can perform synergistic functions (viscosupplementation, anti-inflammatory, bioadhesive) and display distinct levels of structural organization compared to their isolated components [23].

PL407-PL338-HA has also potential to be chondroprotective. Since HA administered as intra-articular injections can enhance the possible regenerative effects of endogenous HA on articular cartilage, restore viscoelasticity of synovial fluid, contribute to HA synthesis by synoviocytes and chondrocytes and prevent degradation of proteoglycans and collagen fibers of extracellular matrix [10,24]. It stimulates metabolism, prevents apoptosis of chondrocytes and inhibits chondral degradation and joint inflammatory responses. These effects of HA therapy are attributed not only to its ability to alleviate symptoms related to osteoarthritis, but also to its interference in the progression of joint degeneration ([11,13,25,95].

Based on the literature, IL-1β and Oncostatin M (OSM) was selected as a model for cartilage breakdown.

This glycoprotein is a pleiotropic cytokine that exerts numerous effects in many different cell types. Some studies have demonstrated that OSM stimulates cartilage proteoglycan resorption and inhibits proteoglycan synthesis in cultured pig cartilage explants in a manner similar to interleukin 1 (IL-1) or tumor necrosis factor α (TNF-α) [5].

The synergistic degradation of cartilage by OSM in combination with either IL-1 or TNF-α has been previously demonstrated in the literature [5,26–29]. OSM has been described in inflammatory processes of the joint in patients with OA and rheumatoid arthritis and it is also known to modulate MEC degradation by controlling the balance between MMPs and the MMPs inhibitor (TIMP) at the site of damage. In addition, it is an enhancer of IL-1β, TNF-α, and interleukin-17 (IL-17) in the progression of cartilage destruction, promoting the production of degradation enzymes, which is an essential cellular mechanism for imitating this pathological condition using *in vitro* models, as used here.

Taken together, the biomaterials, formulation design, and pharmacological aspects all contribute to the innovation reported here, resulting in new hybrid hydrogels capable of favoring the permanence of the drug at the site of injection and thereby minimizing possible systemic side effects, reducing the frequency of injections, and promoting patient compliance. This investigation reports innovative HA/PL hybrid hydrogel systems for delivering SFN, in terms of physico-chemical (supramolecular structure by small angle neutron scattering (SANS), rheological and sol-gel transition properties), biopharmaceutical (drug loading and release mechanisms), and pharmacological (therapeutic efficacy on *in vitro* and *ex vivo* OA models) points of view, envisioning their use for OA treatment by the IA route.

2. Experimental section

2.1. Hydrogel preparation and physico-chemical characterization

For hydrogel synthesis, 20% (m/v) poloxamer (PL, Sigma-Aldrich Chem. Co., St. Luis, USA) solutions, composed of unique (20%) PL407 or PL338, or binary systems composed of PL407-PL338 (10-10%), were prepared by PL dissolution in cold water and maintained at 4 °C under stirring (100 rpm) until a transparent solution was formed [30]. Hyaluronic acid (HA), in power, (from *Streptococcus equi*, MW 1500–1750 kDa, Sigma-Aldrich Chem. Co., St. Luis, USA) (0.05, 0.5 or 1%) and sulforaphane (0.1% SFN, Toronto Research Chemicals, Ontario, CA) were incorporated into the PL solutions at the same conditions as previously described. Formulation designs were carried out by adjusting the PL concentration and its rheological properties.

2.1.1. Chromatographic conditions for SFN analysis

SFN concentrations were determined by HPLC using a system (Ultimate 3000, Chromeleon 7.2 software, Thermo Fisher Scientific, Waltham, USA) composed of a quaternary pump, DAD detector, and C18 column (150 × 4.6 mm, 5 μm; Phenomenex, Torrance, CA, USA). Samples were analyzed at 202 nm, 0.45 mL/min flow rate, at 30 °C. The mobile phase composition was a mixture of acetonitrile and water at 76:24 v/v (%), respectively. The drug retention time was 3.5 min, and 20 μL was used as the sample injection volume. The analytical method was validated according to ICH guidelines, and data represent three experiments in triplicate. The limits of detection (LD, 0.11 μg/mL) and quantification (LQ, 0.3 μg/mL) parameters were calculated from the SFN standard curve (0.5 to 35 μg/mL; $y = 0.634x \pm 0.42$; $R^2 = 0.995$).

2.1.2. Differential scanning calorimetry (DSC) and rheological analysis

For DSC experiments, samples were analyzed using a Q-200 DSC

apparatus (TA Instruments, New Castle, DE, USA). Hydrogel samples were weighed (15 mg), placed in sealed aluminum pans and analyzed in three successive thermal cycles of heating-cooling-heating from 0 to 50 °C, 5 °C/min, using an empty pan as a reference. Thermograms were presented as heat flux (kJ mol^{-1}) *versus* temperature (°C).

Rheological assays were carried out using an oscillatory rheometer (Kinexus Lab., Malvern Instruments, Malvern, UK) with a cone-plate geometry, a temperature range from 10 to 50 °C, and frequency at 1 Hz. Additionally, the temperature was set at 37 °C, and samples were analyzed under a frequency sweep interval from 0.1 to 10 Hz. Parameters related to elastic (G′) and viscous moduli (G″), as well as viscosity (η), were obtained from oscillatory measurements. Data were analyzed by rSpace for Kinexus® software.

2.1.3. Small angle neutron scattering (SANS) experiments

SANS experiments were carried out using the instrument V16 at Helmholtz-Zentrum-Berlin (HZB). The scattering data were recorded at two detector distances: 2 m (wavelength 1.8–3.8 Å) and 11 m (wavelength 1.6–9.2 Å), covering a q range of 0.007–0.5 $Å^{-1}$. Hydrogel samples were prepared in D_2O, placed in quartz glass cuvettes (1 mm light path), and measured at 25 °C and 37 °C. The MANTID data reduction package, adapted to V16, was used to process the SANS data.

2.1.4. Drug incorporation efficiency (IE%), drug loading (DL) percentages, and in vitro release assays

In order to determine the drug incorporation efficiency (IE%), 1 g of hydrogel was solubilized in 4 mL of water and stored at 25 °C, for 24 h. Samples were then centrifuged for 10 min at 13000 ×*g*. Samples of 1 mL of the supernatant were removed, filtered (0.22 μm), and diluted in acetonitrile (1:10 v:v) for SFN quantification by HPLC. Thus, the IE (%) was calculated as the difference between the total SFN concentration and the non-associated drug. The drug loading capacity was calculated according to the equation: DL (%) = incorporated drug concentration / polymer concentration.

SFN release assays were carried out using vertical Franz-type diffusion cells (1.76 cm^2 area, Automatized Microette Plus®, Hanson Research, Chestnut Ridge, NY, USA) with cellulose acetate membranes of MWCO (1000 Da.) as barrier. The donor compartment was filled with 1 g of each formulation and the receptor compartment contained simulated synovial fluid [31] (NaCl 8 g/L, KCl 0.2 g/L, $NaHPO_4$ 1.44 g/L, NaH_2PO_4 0.24 g/L), pH 7.4, at 37 °C, with magnetic stirring (350 rpm). The SFN concentration was determined in aliquots (1 mL) from the receptor compartment, at time intervals from 30 min to 24 h, and analyzed by HPLC. From the results, *in vitro* release profiles were analyzed considering the zero-order, Higuchi, Korsmeyer-Peppas, and Hixson-Crowell models, as described by equations reported in Supplemental Information #1.

2.2. Pharmacological evaluation: in vitro and ex vivo osteoarthritis models

2.2.1. Cell viability assays and the in vitro osteoarthritis model

Cell viability was evaluated in two cell lines, mouse calvarial pre-osteoblast (MC3T3-E1) and human chondrosarcoma (SW1353), that were purchased from ATCC (American Type Culture Collection, Manassas, VA, USA; MC3T3-E1 code CRL2593) and BCRJ (Banco de Células do Rio de Janeiro, Rio de Janeiro, Brazil; SW1353 code BCRJ 03823), respectively. SW1353 cells were cultured in Leibovitz's L-15 medium (Vitrocell, Campinas, SP, Brazil) containing 10% fetal bovine serum (FBS) (Cultilab, Campinas, SP, Brazil) and 100 μg/mL penicillin/streptomycin, and maintained at 37 °C in the absence of CO_2, [5,32,33] while the MC3T3-E1 line was cultured with MEM-alpha medium (MEM-α, Sigma-Aldrich Chem. Co., St. Luis, USA) under similar conditions, with 5% CO_2. Cell cytotoxicity assays were performed according to ISO 10993-5 [34] where hydrogel samples were exposed in direct contact with cell lines and evaluated by 3-(4,5-dimethylthiazol-2-yl)-2,5-diphenyltetrazolium bromide (MTT) reduction and the neutral red (NR) uptake test. The OA *in vitro* model was induced by treatment of SW1353 cells with interleukin 1-β (IL-1β, 10 and 20 ng/mL, Sigma-Aldrich Chem. Co., St. Luis, USA) as previously described [33,35,96,97]. The NF-κB p65, cyclooxygenase 2 (COX-2), and type II collagen protein expression levels were evaluated by *western blot* analysis for inflammatory process indicators. The experimental protocol is detailed in Supplemental Information #2.

2.2.2. Ex vivo cartilage degradation assay, glycosaminoglycan quantification and histological evaluation

For the cartilage explant model, metacarpal and metatarsophalangeal joints were extracted from adult pigs (with 5–6 months and 110–120 kg) purchased from a slaughterhouse certified by Brazilian Federal Inspection Service No. 2259 (Angelelli Frigorífico Ltda., Piracicaba, SP, Brazil). The protocol was approved by the Federal University of ABC Institutional Animal Care and Use Committee, in accordance with the Guide for the Care and Use of Laboratory Animals (#87190103/18).

The joints were excised for cartilage separation, and selected cartilage samples (3 slices, each of with 3 mm^2) were cultured in a 24-well tissue culture plate with DMEM (Sigma-Aldrich Chem. Co., St. Luis, USA) containing penicillin (200 units/mL), streptomycin (200 mg/mL), and gentamicin (50 μg/mL). Explants were maintained in a humidified incubator with 5% CO_2 at 37 °C. Cartilage degeneration was induced with recombinant human IL-1β (20 ng/mL, Sigma-Aldrich Chem. Co., St. Luis, USA) plus human Oncostatin M (OSM, 25 ng/mL, Sigma-Aldrich Chem. Co., St. Luis, USA) [5] and were then treated with PL407/PL338, HA + PL407/PL338 + SFN, or SFN. DMEM and dexamethasone (DEXA, 25 nM) were used as untreated and treated controls, respectively. Explants were cultured for 21 days, the medium collected, replaced every 7 days and analyzed for sulfated glycosaminoglycans (S-GAGs) and uronic acid (UA) quantification. Quantification protocols are detailed in Supplemental Information #3.

After 21 days, cartilage explants were washed with phosphate buffer, embedded in special inclusion medium for freezing of biological samples (Tissue-Tek O.C.T. Compound, Sakura-4583) and maintained at −20 °C. Ultrafine sections (5 μm) were created using a cryostat (Leica CM1950, Wetzlar, Germany), stained with Hematoxylin and Eosin (HE), and analyzed under light microscopy (Axiovert A1, Zeiss, Jena, Germany).

2.3. Statistical analysis

All experiments were carried out in triplicate, and results are presented as mean ± S.D. Experimental data were analyzed by GraphPad Prism software, (GraphPad Software Inc., La Jolla, CA, USA). ANOVA (one and two-way) were used for comparison among groups, followed by Tukey-Kramer *post hoc* test or Student's *t*-test. Statistical significance was defined as $p < 0.05$.

3. Results and discussion

3.1. Physico-chemical characterization

3.1.1. Differential scanning calorimetry and rheological assays: hydrogel thermodynamics and viscoelastic properties

Thermograms displayed endothermic peaks with slight displacement, related to the differences on polymers final concentrations and hydrogels compositions. Table 1 shows results from micellization temperature (Tm, °C) and the enthalpy change (ΔH°, cal/g) analysis comparing the associations between HA and PL-based hydrogels, before and after SFN incorporation.

In general, the Tm values were similar among PL407 hydrogels formulations, being around 17 °C, but for PL338 (20) based systems, it was observed an increase on Tm (23 °C) and a decrease in the ΔH° values. On the other hand, PL407-PL338-based binary systems revealed

Table 1
Values referring to micellization temperatures (Tm). enthalpy (ΔH). G′ (Elastic). G″ (Viscous) moduli. Viscosity (η. mPa·s) at 25 °C and 37 °C and sol-gel transition temperatures (Tsol-gel) relative to PL 407/10–14.14 17.27 30.4 0.55.

Formulations (F. % m/v)	Additives (% m/v)	Tm (°C)	ΔH (cal/g)	T sol-gel (°C)	G′ (Pa)	G″ (Pa)	G′/G″ (at 1 Hz)	η* (×10^3. 25 °C)	η* (×10^3. 37 °C)
	–	17.3	0.83	27	10,600	573	18.5	0.153	1690
	SFN	16.8	1.02	28	8988	535	16.8	0.097	1433
	HA 0.05	16.6	0.83	27	8416	465	18.1	0.155	1341
PL407	HA 0.05-SFN	17.2	0.83	28	7914	493	16.1	0.138	1262
(F1. 20)	HA 0.5	16.3	0.63	27	9678	783	12.4	1.025	1070
	HA 0.5-SFN	16.4	0.98	28	9767	731	13.5	1.246	1411
	HA 1	17.0	0.87	26	8055	476	16.9	2.667	1284
	HA 1-SFN	17.0	0.87	27	7542	493	15.3	2.595	1203
	–	23.0	0.44	36	3905	1082	3.6	0.335	644.9
	SFN	23.0	0.51	36	3350	955	3.5	0.354	554.4
	HA 0.05	23.0	0.47	36	781	307	2.5	0.649	133.5
	HA 0.05-SFN	23.0	0.53	37	672	256	2.6	0.644	114.5
	HA 0.5	22.5	0.75	37	771	270	2.8	0.240	106.6
	HA 0.5-SFN	22.0	0.61	37	820	320	2.6	0.538	127.6
PL338	HA 1	22.4	0.42	34	6342	600	10.6	4.9	1023
(F2. 20)	HA 1-SFN	22.2	0.55	35	6303	640	9.9	2.4	693.2
	–	18.2	0.68	33	5130	1105	4.6	0.374	835.2
	SFN	18.6	0.52	33	6700	1215	5.5	0.406	1084
	HA 0.05	18.5	0.63	33	3754	907	4.1	0.56	614.2
	HA 0.05-SFN	18.9	0.52	33	4804	1012	4.7	0.76	781.4
	HA 0.5	18.4	0.72	33	4004	768	5.2	6.54	811.0
	HA 0.5-SFN	18.7	0.51	33	5644	844	6.7	7.64	908.3
	HA 1	17.4	0.43	32	6619	794	8.3	21.9	1061
PL407-PL338 (F3. 10-10)	HA 1-SFN	17.7	0.62	32	6331	802	7.9	22.0	1016

intermediate values for Tm and AH°, where we have noticed the greater influence of PL338 insertion into the micellization process [23,36]. Similar results were also observed by other authors, considering that the association kinetics among three systems are different, since the micelles formation involves the dehydrating process of PPO blocks and the micelles dissociation are dependent on the hydration of the same blocks [37,38].

PL407 (20) systems showed higher ΔH° values (0.83 cal/g) compared to PL338 (20) (0.55 cal/g) and PL407-PL338 (10-10) (0.68 cal/g). This effect was clearly detected since all hydrogels were prepared at the same polymer final polymer concentration to observe the influence of PL-type as unique and binary systems. In a similar manner, the addition of SFN to PL407, PL338 and PL407-PL338 systems reduced the enthalpy variation, disturbing the systems self-organization by insertion of the drug into the hydrogels. In fact, SFN has an amphiphilic structure with water solubility of 2.5 mg/mL partition coefficient (log P octanol/water) of 0.45 [39], so although this drug is soluble in water, it has also a high affinity for organic phases. Thus, it is expected that SFN would be partially inserted between the hydrophobic core and the hydrophilic corona, thereby interacting with their respective polar and apolar groups into the micellar systems.

On the contrary, the presence of HA different concentrations and the addition of the SFN into the hybrid systems did not significantly change the parameters related to the micellar aggregation process, showing that they do not interfere on hydrogels thermoreversible properties. In addition, no HA concentration-dependent effects were observed even after SFN incorporation, indicating the components compatibility and the maintenance of thermoreversible properties for all PL-based compositions.

Similar results were also reported by Mayol et al. [20] when developed a hybrid PL407-PL188 (18-18%) hydrogel containing 1 and 2% HA, for improving the formulations mechanical properties, their bioadhesive and water permeability properties. DSC analyzes performed in this study, a decrease on the water fraction interacting with polymers was observed in the thermograms according to the highest HA content into the hydrogels. This result suggests that the addition of HA in PL gels disturbs the water-PL while favors PL-PL interactions, allowing the formation of a possible more organized hydrogel structure.

Rheological analysis provided essential parameters for evaluating the hydrogels mechanical properties. Elastic (G′) and viscous (G″) moduli, viscosity (η) and sol-gel transition temperature (Tsol-gel) and G′/G″ relationship were determined for all hydrogels formulations considering the incorporation of additive s such as HA and/or SFN. Representative rheograms and numerical results are presented on Fig. 1 and Table 1, respectively.

In general, the incorporation of 0.05 or 0.5% HA did not shift the Tsol-gel, but differences were observed after comparisons between both PL type containing 1% HA, since Tsol-gel (27 °C) values for PL407 were lower in relation to PL338 (34 °C) and PL407-PL338 (32 °C) hydrogels. In fact, the differences on hydrophilic lipophilic balances (HLB) between PL338 (HLB = 28) and PL407 (HLB = 22) provided the formation of binary systems with lower viscosity and G′/G″ relationship values that observed for PL407-based hydrogels, suggesting a possible structural reorganization according to HA concentration and PL hydrophobicity, related to an increase on micellar packaging surrounded by HA into the hydrophilic intermicellar spaces [23,40,41]. This type of organization was also proposed by Sosnik and Cohn [42] and Mayol et al. [20] suggesting that the PL-HA interactions occur due to secondary bonds, such as hydrogen bonds, between the hydrophilic (hydroxyl and carboxylic) groups of HA and the PEO units of the micellar corona.

Additionally, it is necessary to emphasize the essential role of the PL407-PL338 binary composition for structuring hydrogels with Tsol-gel close to physiological and forming resistant systems to degradation with adequate mechanical properties, which can be seen for all binary hydrogels. The presence of SFN and HA into PL407-PL338 did not alter the formulations stability.

It is recommended that for the development of *in situ* gelling systems for injectable use, formulations must be structurally liquid-viscous. In this case, formulations prepared here displayed elastic modulus (G′) values from ~8 to 18 times higher than those observed for the viscous modulus (G″), favoring the hydrogels formation. Those results are in agreement with other reports that demonstrate the predominance of the viscoelastic behavior, an essential property for developing adequate injectable hydrogels formulations (Zhang et al., 2008; [23,37,43–46]).

3.1.2. Hydrogel supramolecular structure and phase organization determined by small angle neutron scattering (SANS)

Fig. 2(A and B) shows SANS scattering patterns and the structural phase organizations of the hydrogels at 25 °C and 37 °C (both considered as storage and physiological temperatures, respectively).

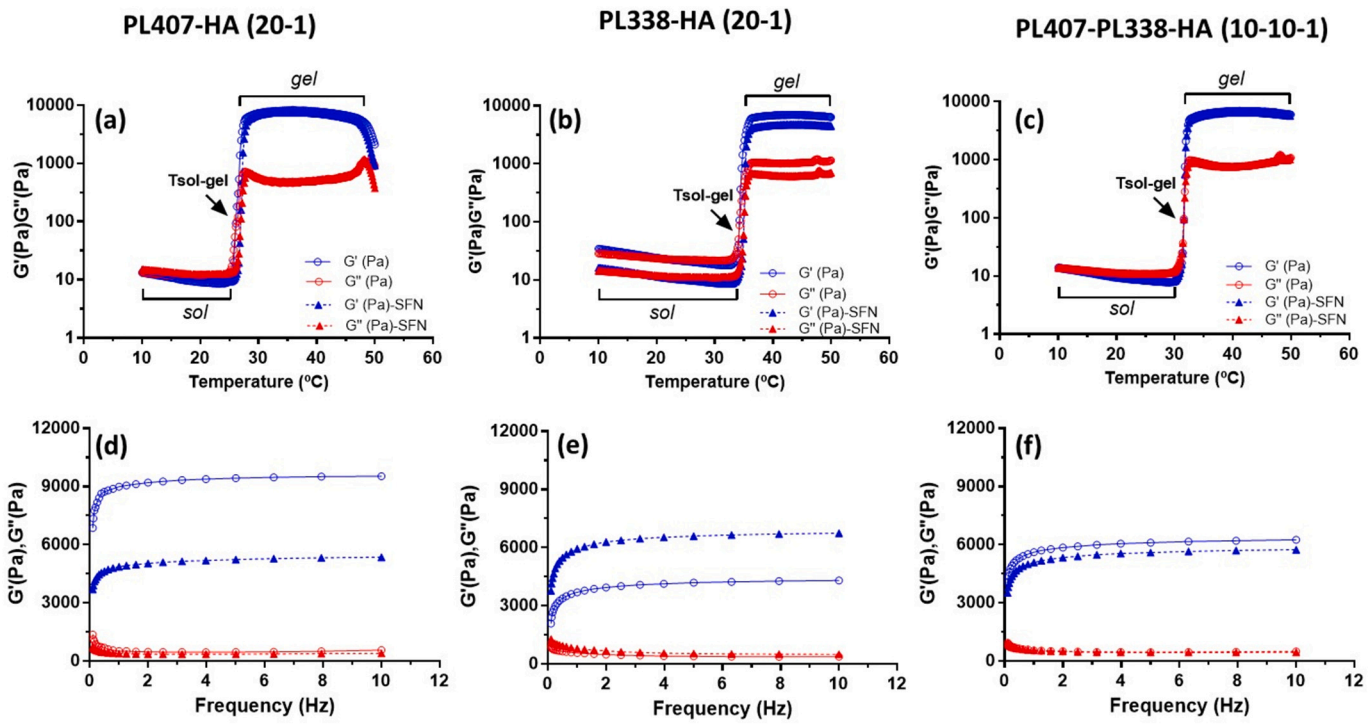

Fig. 1. Representative rheograms for PL407 (20%), PL338 (20%), PL407-PL338 (10-10) with HA (1%), before and after SFN (0.1%) incorporation as function of temperature and frequency sweep analysis. Arrows represent sol-gel transition temperatures (Tsol-gel).

At 25 °C, the systems composed of PL338 revealed Porod's coefficient values of −1.37, −1.21, −1.30, and −1.33 for PL338, PL338-SFN, PL338-HA, and PL338-HA-SFN, respectively. For PL338-HA, there was agglomeration of the particles at a very low angle, indicated as an increasing on the scattering signal, while a lamellar phase organization with a planar distance (d_{10}) parameter of 214.88 (5) Å was observed for all compositions at 37 °C. In addition, the Porod's coefficients for the PL338 systems were −1.52 (PL338), −1.57 (PL338-SFN), −1.70 (PL338-HA), and −1.59 (PL338-SFN-HA), which were slightly higher than that observed at 25 °C, indicating an increase in the surface fractality of the particles.

For the PL407 unique systems (at 25 °C and 37 °C, Fig. 2B), the hydrogel phase organization remained unchanged: lamellar, with parameter d_{10} = 214.88 (5) Å for all compositions and both temperatures. In this case, the Porod's coefficients were −1.84 (PL407), −1.68 (PL407-SFN), −1.66 (PL407-HA), and −1.94 (PL407-SFN-HA) at 25 °C, while slightly differences were observed at 37 °C, with values of −1.93 (PL407), −1.9 (PL407-SFN), −1.89 (PL407-HA), and −1.8 (PL407-SFN-HA).

In the case of PL407-PL338 hybrid systems, the structures at 25 °C presented as hexagonal structures with parameter d_{10} = 185.62 (5) Å for all compositions, both in the presence and absence of SFN and HA. The Porod's coefficients observed at 25 °C for these systems were −1.64 (PL407-PL338), −1.63 (PL407-PL338-SFN), −1.5 (PL407-PL338-HA), and −1.39 (PL407-PL338-SFN-HA). Remarkably, increasing the temperature to 37 °C, resulted in a transition to different cubic phase type organizations, depending on the additives present (HA or SFN). For PL407-PL338, the system structure was cubic Fd3m with lattice parameter a = 321.50 (5)Å (here the Bragg peaks corresponded to spacing ratios $\sqrt{3} : \sqrt{8} : \sqrt{11} : \sqrt{12}$…). Similar profiles were observed for PL407-PL338-SFN, where the structure remained cubic Fd3m with the same lattice parameter value. However, for the PL407-PL338-HA systems, the phase organization changed to cubic Pm3n with lattice parameter a = 262.50 (5)Å, where the Bragg peaks corresponded to spacing ratios $\sqrt{2} : \sqrt{4} : \sqrt{5} : \sqrt{6} : \sqrt{8} : \sqrt{10}$…. In contrast, in the presence of both SFN and HA in the PL407-PL338 system, the structure changed to cubic Im3m with lattice parameter a = 262.50 (5)Å, where the Bragg peaks were identified by spacing ratios $\sqrt{2} : \sqrt{4} : \sqrt{6} : \sqrt{8} : \sqrt{10} : \sqrt{12}$…. Furthermore, the Porod's coefficients for these cubic systems indicated an increasing in fractality: −1.86 (PL407-PL338), −1.95 (PL407-PL338-SFN), −2.03 (PL407-PL338-HA), and −1.68 (PL407-PL338-SFN-HA).

SANS scattering patterns revealed a differential structural behavior for hydrogels according to the PL type and presence of HA and SFN. In fact, the increase in fractality and the transition between different types of cubic phase organization were important evidence of the interactions of components. For the PL338 unique systems, the surface fractality suggests possible interactions between PEO and HA hydroxyl groups on the micellar hydrophilic corona, resulting in highly hydrated systems. On the other hand, systems composed of PL407, a more hydrophobic polymer (HLB = 22) compared to PL338 (HLB = 28), displayed a lamellar phase organization in the presence of HA and SFN, indicating the influence of the polymer type on the structural organization of the hydrogel and the formation of a crystalline matrix. In a previous study by SAXS, we reported that the formation of hexagonal phase organization for PL-HA hydrogels was observed by using 0.025% and 0.05% HA. However, it was observed that the incorporation of higher HA concentrations (0.5% and 1%) and an amphiphilic drug, such as SFN, maintained the lamellar system structure in a different way to that described before, where the addition of hydrophobic drugs (such as lidocaine base) [23] or as salt forms (sumatriptan succinate) [37,43,44,98] induced the formation of hexagonal structures and sustained drug release. Regarding the PL407-PL338 systems, according to literature, the cubic forms Fd3m (for PL407-PL338 and PL407-PL338-SFN) and Pm3n (for PL407-PL338-HA) consist of micelle packing, and the Im3m parameter (as observed for the PL407-PL338-SFN-HA system) indicated a viscous bicontinuous cubic phase formation, in agreement with rheological properties, as evidenced by $G' > G''$ and the high viscosity values, which were observed for all binary systems. Considering their inherent structural complexities, bicontinuous systems present wide applicability as drug delivery systems, being characterized by networks composed of

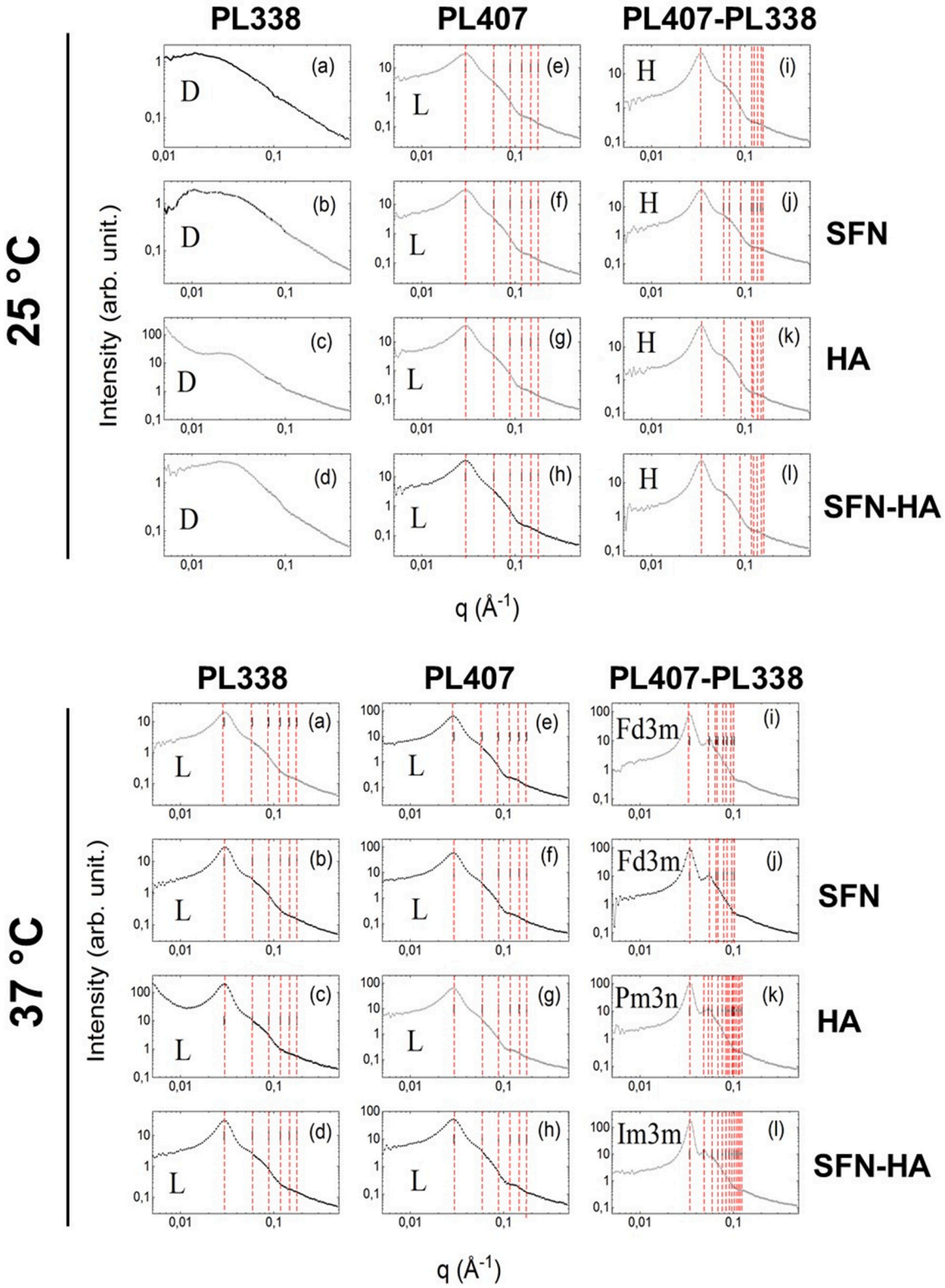

Fig. 2. SANS patterns for PL407 (20%), PL338 (20%) and PL407-PL338 (10-10) isolated or in association with SFN (0.1%) and HA (1%). Scans show different types of phase organization compressing lamellar (L), hexagonal (H) and cubic types (Fd3m, Pm3m, Im3m) at 25 and 37 °C.

continuous bilayers and water channels, while micellar cubic phases are formed by micelles organized as cubic lattices, [47,48], for example Fd3m, observed for PL407-PL338-SFN, which was shifted to Im3m into PL407-PL108-SFN-HA. Those types of cubic phase organization are characterized by stable and hydrophilic clusters assembled as interpenetrating channels [49], allowing a possible structural model made of central PL-based mixed micelles surrounded by an HA network hydrophilic matrix to be built, with SFN amphiphilic molecules dispersed into both the micellar and network phases, and the interpenetrating water channels (Fig. 2). Due to this phase organization shift, or even coexistence, it is possible to modulate the sustained drug release profile for each system.

3.1.3. Drug incorporation efficiency (IE%), loading percentages (DL%), and in vitro release assays: formulation design and release mechanisms

The incorporation efficiency of SFN ranged from 76% to 92%, according to the formulation composition and HA concentration. The unique PL-based systems (PL407 and PL338) and the PL407-PL338 binary system showed similar IE% (76% to 80%), but the incorporation of 0.5% and 1% HA increased the SFN incorporation efficiency to 85% and 92%, respectively, with $p < 0.01$ and $p < 0.001$. The drug loading

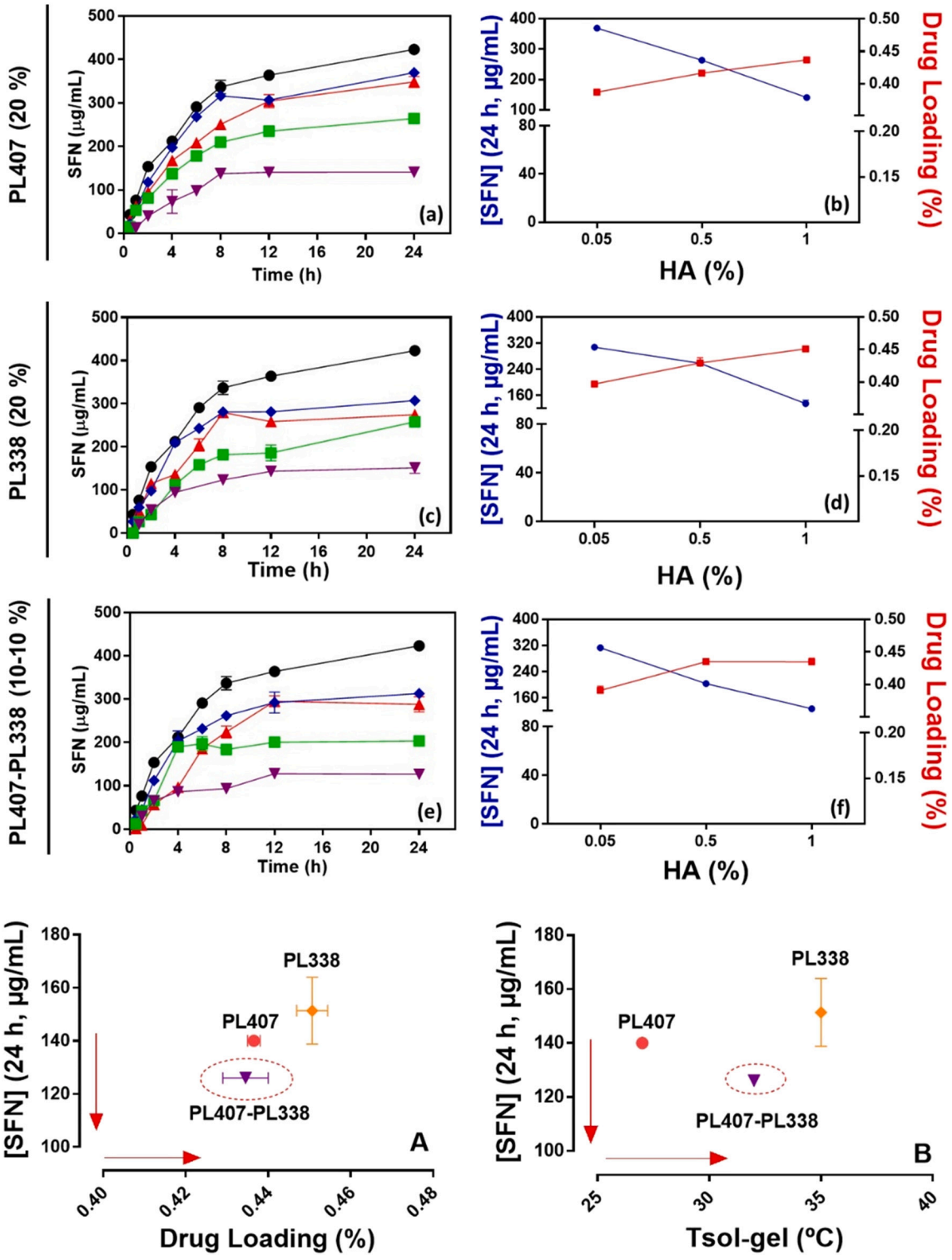

Fig. 3. Sulforaphane (SFN) release profiles (a, c, e), drug loading percentages and SFN released concentrations (at 24 h) relationships against different HA concentrations (b, d, f). Drug release profiles were presented for PL407 (20%, a, b), PL338 (20%, c, d) and PL407-PL338 (10-10%, e, f) in the presence or absence of HA (1%). Relation between SFN concentrations released with drug loading percentage (A) and sol-gel temperatures (B) for different formulations containing HA 1%. Dash circles were used to select hydrogels systems considering the best performance for both parameters (drug loading and Tsol-gel). Data expressed as mean ± S.D. ($n = 6$/formulation). (●) 1 mg/mL SFN in water; (▲) PL407 20%; PL338 20% or PL407-PL338 10-10%; (◆) PL407 20%; PL338 20% or PL407-PL338 10-10% with HA 0.05; (■) PL407 20%; PL338 20% or PL407-PL338 10-10% with HA 0.5; (▼) PL407 20%; PL338 20% or PL407-PL338 10-10% with 1%.

percentages were ~0.39 for PL407, PL338, and PL407-PL338, while the systems containing 1% HA gave DL values of 0.42, 0.43, and 0.45 for PL407, PL338, and PL407-PL338, respectively. SFN release profiles from the different hydrogel formulations are shown on Fig. 3(A, C, E) and Table 2. The drug release in aqueous solution (0.1% or 5.6 mM) was linear until 8 h, reaching maximum values up to 12 h. The formulations composed of unique or binary systems of PL407 and PL338 modulated drug release, evoking a sustained profile with SFN concentrations values (at 24 h) of 348.4 ± 12.6 μg/mL (PL407), 274.8 ± 13 μg/mL (PL338), and 288 ± 7.6 μg/mL (PL407-PL338). The presence of the highest HA concentration (1%) showed SFN release concentrations of 140.8 ± 1.5 μg/mL (PL407), 151.3 ± 2.6 μg/mL (PL338), and 126.7 ± 1.8 μg/mL (PL407-PL338), reducing the drug release from 1.8 to 2.4-times compared to HA-free systems ($p < 0.001$). This pronounced effect can be attributed to the formation of a highly structured polymeric network organized as bicontinuous cubic phases, as evidenced by SANS analysis, evoking surface interactions with PL-micelles and forming a hydrophilic matrix in the intermicellar spaces, capable of sustaining SFN release. These observations are also in agreement with other reports in the literature [20,21,23,50,92].

The mathematic model that best described the SFN release profiles was Korsmeyer-Peppas, based on the highest correlation coefficients ($R^2 = 0.85 \geq 0.96$), with n values from 0.48 to 0.89 for most of the formulations, as observed in Table 2, being described as anomalous and super case-II kinetics, associating diffusion and erosion mechanisms to evoke SFN release from the hydrogels.

Considering the physico-chemical and biopharmaceutical properties described before, the main parameters used for the formulation design of the hydrogels were: i) concentration and influence of HA; ii) influence of concentration and type of PL; iii) drug loading capacity (DL); iv) Tsol-gel; and v) release constant (Krel) values. Fig. 3(B, D, F) shows representative relationships among the different concentrations of HA (0.05, 0.5 and 1%) with the SFN concentration released in 24 h and the percentage of DL. As ideal features for nanocarrier systems, the greater capacity for drug loading associated with low drug Krel values were considered when selecting formulations containing 1% HA for the *in vitro/ex vivo* assays, as the most promising SFN delivery systems.

According to the main parameters considered, a low drug release concentration at 24 h was associated with high drug loading percentage and a Tsol-gel close to physiological conditions, indicated by the arrows in Fig. 3A and B. Although other formulations showed similar SFN concentrations released at 24 h (~130 μg/mL) and DL percentages (from 0.45 and 0.43%), it is known that one of the main requirements for a thermoreversible gel to be used as an injectable formulation is a liquid form before administration, becoming a soft-gel after injection, under physiological conditions (37 °C). Therefore, the PL407-PL338-HA-SFN system was selected to perform *in vitro* and *ex vivo* assays in OA models.

3.2. In vitro and ex vivo pharmacological evaluation

3.2.1. Cell viability assays

The cell viability evaluation was performed in SW1353 (primary grade II chondrosarcoma), by MTT and NR assays. Cytotoxicity assays were performed by varying the concentrations of SFN, PL407-PL338, PL407-PL338-SFN, and PL407-PL338-HA-SFN. The viability using the cell line MC3T3-E1 (pre-osteoblastic) was performed only for complete system (PL407-PL338-HA-SFN) by NR assays (Fig. 4E).

The quantitative MTT assay was used for the evaluation of cell viability, but there is substantial evidence that SFN acts indirectly to increase the antioxidant capacity of animal cells and their ability to deal with oxidative stress, although it is not a direct pro-oxidant or antioxidant [51]. Ye and Zhang [52] found that glutathione, a signaling molecule that maintains redox balance and protects cells from reactive oxygen species, increased 4.3 times more in human liver tumor cells as a result of SFH [52]. As MTT is a test based on an oxidation-reduction reaction, it was considered possible that SFN could affect the MTT reduction and lead to imprecise cell viability evaluation results. To confirm such an assumption, SFN cytotoxicity assays were performed using both MTT and NR tests (Fig. 4).

Fig. 4A shows the cell viability percentages after treatment with different SFN concentrations, using the MTT test in SW1353 cells. It is assumed that an agent can be considered cytotoxic if cell viability is lower than 70% [34]. This assay provides an evaluation [53–55], with statistical differences only being observed for 50 μM SFN (56 ± 9.1% cell viability).

On the other hand, evaluation by the NR uptake test in SW1353 cells showed percentages of 83 ± 10.6%, 76 ± 8.4%, 68 ± 10.2%, and 40 ± 12.6% for 5, 10, 20, and 50 μM SFN concentrations, respectively, with concentration-dependent behavior (Fig. 4B). NR is a cationic marker, which is internalized by cells through cell membrane diffusion, being directed towards lysosomal organelles [56–58]. In this sense, results from the NR uptake assay were different in relation to those obtained by MTT, demonstrating its greater sensitivity for SFN cytotoxicity evaluation. Thus, the NR uptake test was selected for the evaluation of cell

Table 2
SFN release constants (Krel) and determination coefficients (R^2) obtained for non-incorporated SFN (0.1%), PL407 or PL338 (10, 18 or 20%) and HA (0.05, 0.5 or 1%).

Formulations (% m/v)	Zero order		Higuchi		Korsmeyer-Peppas			Hixson Crowell	
	K_0 (mM·h^{-1})	R^2	K_H (mM·h$^{-1/2}$)	R^2	K_{KP} (mM·h^{-n})	R^2	n	K_{HC} (mM·h$^{-1/3}$)	R^2
SFN (0.1)	15.3	0.75	95.6	0.92	79.4	0.94	0.61	0.14	0.62
PL407 (20)	13.2	0.80	80.9	0.95	58.8	0.96	0.64	0.14	0.67
PL407-HA (20-0.05)	13.8	0.69	87.5	0.88	54.9	0.91	0.74	0.15	0.56
PL407-HA (20-0.5)	9.90	0.74	62.0	0.91	41.6	0.91	0.71	0.13	0.58
PL407-HA (20-1)	5.05	0.59	34.8	0.78	19.9	0.85	0.77	0.10	0.51
PL407 (18)	12.2	0.77	75.4	0.93	45.7	0.95	0.72	0.15	0.63
PL407-HA (18-0.05)	11.6	0.72	72.6	0.90	46.7	0.93	0.71	0.14	0.59
PL407-HA (18-0.5)	10.3	0.74	64.2	0.92	46.7	0.93	0.67	0.13	0.60
PL407-HA (18-1)	4.50	0.60	30.1	0.78	43.6	0.82	0.48	0.07	0.52
PL338 (20)	10.3	0.61	67.1	0.81	39.8	0.84	0.79	0.14	0.49
PL338-HA (20-0.05)	11.1	0.61	72.1	0.82	50.1	0.91	0.66	0.13	0.52
PL338-HA (20-0.5)	10.4	0.80	63.5	0.94	31.6	0.93	0.75	0.19	0.50
PL338-HA (20-1)	4.70	0.64	31.7	0.82	30.2	0.86	0.60	0.08	0.55
PL407-PL338 (18-2)	9.40	0.70	58.8	0.87	36.3	0.95	0.89	0.13	0.58
PL407-PL338-HA (18-2-0.05)	9.60	0.70	60.5	0.87	50.1	0.98	0.71	0.12	0.60
PL407-PL338-HA (18-2-0.5)	6.22	0.68	39.3	0.87	31.6	0.92	0.84	0.11	0.54
PL407-PL338-HA (18-2-1)	4.13	0.57	28.3	0.75	25.1	0.93	0.75	0.08	0.53
PL407-PL338 (10-10)	12.9	0.72	80.8	0.88	10	0.89	1.33	0.20	0.57
PL407-PL338-HA (10-10-0.05)	11.5	0.65	74.3	0.85	50.1	0.91	0.70	0.14	0.53
PL407-PL338-HA (10-10-0.5)	7.03	0.45	48.1	0.67	31.6	0.83	0.73	0.11	0.41
PL407-PL338-HA (10-10-1)	3.60	0.69	23.9	0.83	31.6	0.86	0.43	0.07	0.59

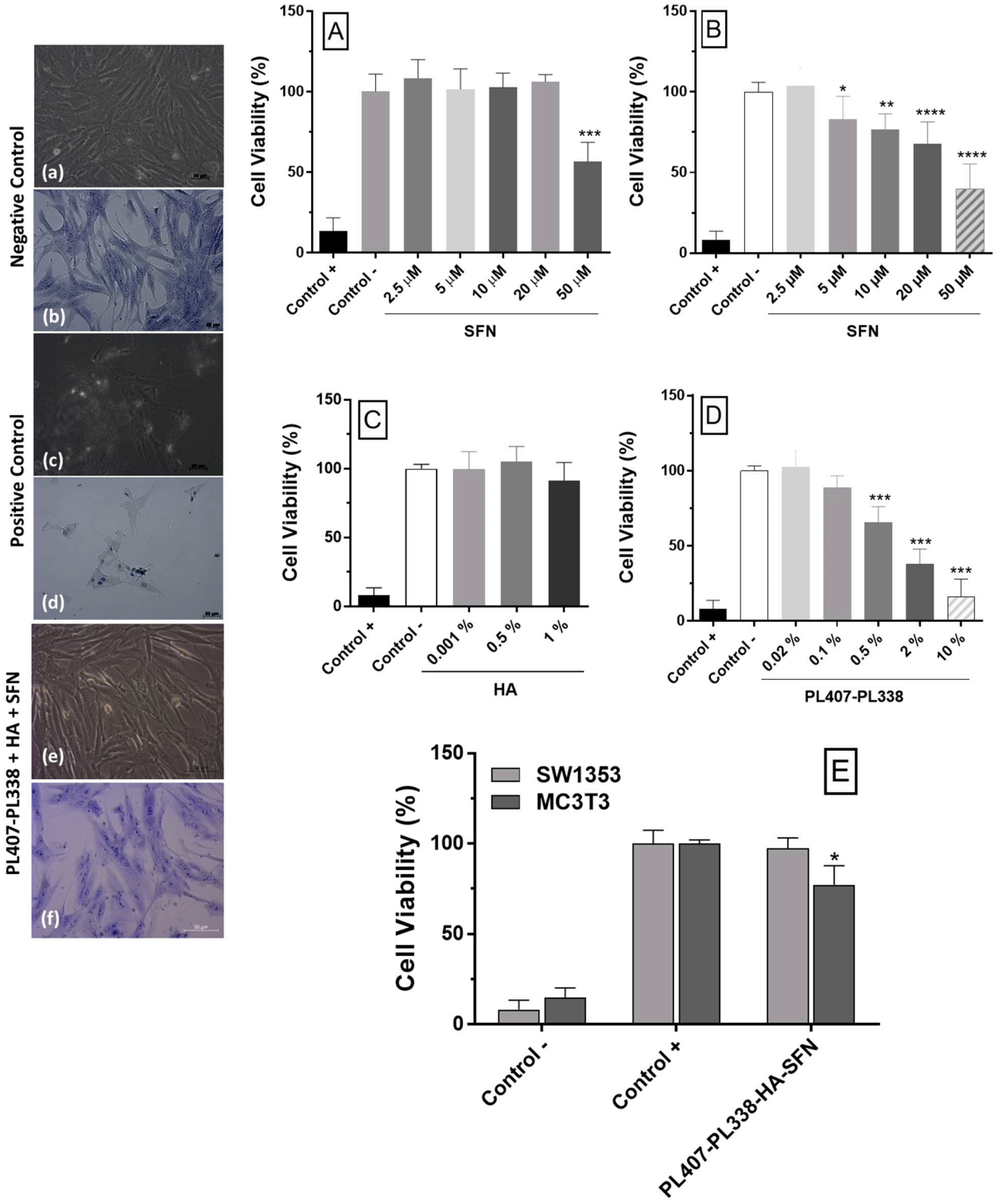

Fig. 4. Cell viability percentages after treatment with different PL-based formulations. After 24 h of incubation with negative (cells treated with culture medium, a- no coloration and b – toluidine blue stain), positive (phenol 0.25%, c- no coloration and d – toluidine blue stain) and hydrogel formulation (e- no coloration and f – toluidine blue stain). Viable cells percentages after treatment with SFN evaluated by MTT reduction (A) and NR uptake (B) assays; HA (C); PL 407-PL338 (D) by NR uptake assay. SW1353 and MC3T3 cells lines viability after treatment with PL407-PL338-HA-SFN by NR uptake test (E). Data were expressed as mean ± S.D. from three independent experiments in triplicate and analyzed by one-way ANOVA followed by Tukey-Kramer post-test. *** $p < 0.001$; ** $p < 0.01$; * $p < 0.05$. PL407-PL338, HA and SFN concentrations were 0.035%, 0.001% and 10 μM, respectively. (For interpretation of the references to colour in this figure legend, the reader is referred to the web version of this article.)

viability for all hydrogel formulations.

For PL407-PL338 hydrogels, the mean cell viability (SW1353) percentages ranged from 102 ± 8.9% to 16 ± 9.5%, at 0.02% and 10% final concentrations, respectively. At 0.5%, 2%, and 10% PL407-PL338, a significant difference ($p < 0.001$) was observed in relation to the negative control, as well as an increase in the cytotoxic effects in response to high polymer concentrations (Fig. 4C). However, the cell viability values for different concentrations of HA (Fig. 4D) and the final formulation (PL407-PL338-HA-SFN) (Fig. 4E) exceeded 90% of cell viability, showing no statistical differences when compared to the negative (non-cytotoxic) control. MC3T3 cells were also treated with the final formulation, PL407-PL338-HA-SFN, with cell viability values above 75% being observed (Fig. 4E). These results corroborated those obtained for the SW1353 cell line, highlighting the non-cytotoxicity of the PL407-PL338-HA-SFN system.

In another analysis, SW1353 cells were evaluated by light microscopy, for a morphological cytotoxicity assessment after treatment. The negative, non-cytotoxic control showed a confluent cell monolayer, typically fibroblastic, according to their growth pattern. The cells were quite scattered and elongated, without the presence of debris or evidence of degeneration. After the addition of phenol (0.25%), cellular debris and its suspension were observed in the positive control, which is a typical cytotoxic response.

Morphological analysis revealed that cells treated with PL407-PL338-HA-SFN evoked a growth pattern like that obtained for the negative control, as a confluent monolayer without vacuolization or signs of cellular degeneration. Thus, the morphological analyses are in agreement with the quantitative NR assay. There are no studies describing cytotoxic evaluation of PL, HA, and SFN compounds in SW1353 cells, which shows the relevance of the present work, since the non-toxicity of these compounds has already been reported in the literature for other cells types [9,11,24,59,60,99].

3.2.2. *In vitro pharmacological evaluation: osteoarthritis model in SW1353 cells*

Inflammation has been recognized as an essential process in the pathogenesis of OA, since IL-1β is released by activated synoviocytes or chondrocytes, followed by the induction and activation of NF-κB, activator Protein 1 (AP-1) and MAPK signaling. In this sense, SW1353 cells also exhibit these signaling pathways [61,62]. IL-1β treatment in chondrocytes and SW1353 cells causes activation of MAPKs and AP-1 [63,64], which associated to the activation of NF-κB pathway, induce inflammation-related gene and protein expression [32,35]. Thus, SW1353 cells stimulated with IL-1β were used in this study as an *in vitro* cellular OA model of OA. SW1353 cells were pretreated for 24 h with PL407-PL338, HA, and SFN, either isolated or in association, and the culture medium containing 10 ng/mL IL-1β was then added. Protein expression levels of NF-κB p65, COX-2, and type II collagen were evaluated using western blot analysis.

In general, IL-1β increased the expression of NF-κB p65 and COX-2 proteins but decreased the expression of type II collagen in relation to the control (untreated) (Fig. 5). Pretreatment with the formulation and non-encapsulated SFN inhibited cytokine-mediated effects, thus promoting a significant decrease in NF-κB p65 (Fig. 5A) and COX-2 (Fig. 5B), as well as increased type II collagen (Fig. 5C) protein expression.

Pro-inflammatory mediators, such as IL-1β, lead to induction of NF-κB signaling pathway, which enhances the articular damage through induction of nitric oxide (NO), cyclooxygenase 2 (COX-2), nitric oxide synthase (NOS) and prostaglandin E2 (PGE2), promoting synthesis of catabolic factors, cartilage inflammation and apoptosis of OA chondrocytes [33,35]. Several studies have demonstrated that SFN exhibits anti-inflammatory activity by inhibiting NF-κB translocation, a mechanism that disrupts inflammatory signals to the nucleus [65]. Inhibition of IKB phosphorylation and/or degradation, IKK phosphorylation, and NF κB nuclear translocation by SFN are described in various cell types, including chondrocytes [5,66]. In the present study, PL-HA-SFN based treatment was able to reduce NF κB-p65 expression and, consequently, decreased COX-2 levels in IL-1β-stimulated SW1353 cells. These results indicated that the protective and anti-inflammatory effects of SFN on human SW 1353 chondrosarcomas may occur *via* the NF κB pathway.

Considering that cartilage destruction is a fundamental process on OA progress, the role type II-collagen was further explored. The SW 1353 human chondrosarcoma cell line has been employed in several studies as *in vitro* model to investigate the molecular mechanisms and pharmacological treatments for OA, due to its similarity with human OA chondrocytes [33,100]. IL-1β is thought to play a major role in inflammatory and destructive processes associated with the breakdown of cartilage matrix in OA. This cytokine suppresses the expression of cartilage-specific collagens [67–69] and proteoglycans [70] in cultures

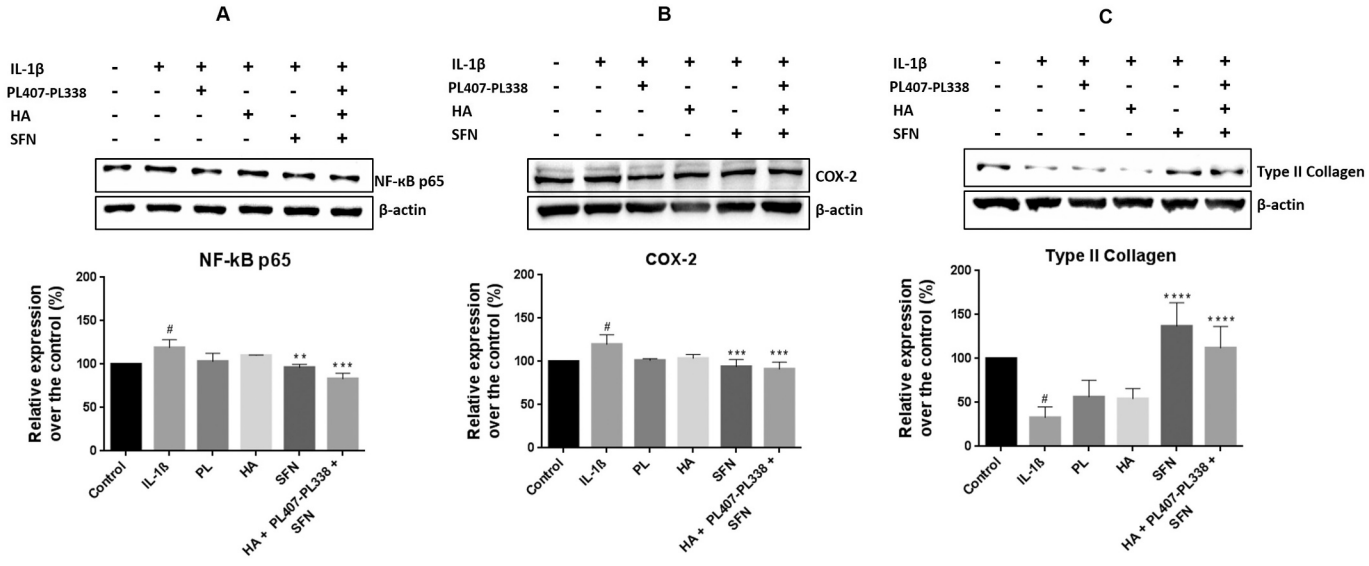

Fig. 5. Effects of PL-HA-SFN formulations on NF-κB-p65, COX-2 and type 2-collagen expressions levels by IL-1β-stimulated SW1353 cells. Cells were pretreated with 0.035% PL407-PL338, 0.001% HA and 10 μM SFN, isolated and in association (24 h). NF-κB-p65 (A), COX-2 (B) and Type 2-collagen (C) expression levels were determined by western blot analysis. Data were expressed as mean ± standard deviation from three independent experiments in triplicate and analyzed by one-way ANOVA followed by Tukey-Kramer post-test. #$p < 0.05$ *vs.* control group; **$p < 0.01$ *vs.* IL-1β treated group; ***$p < 0.001$ *vs.* IL-1β treated group.

of chondrocytes and intact cartilage. IL-1 may also have a role during inappropriate cartilage matrix repair that accompanies inflammatory joints disorders by stimulating the synthesis of non-cartilage collagens (type I and type III) by chondrocytes [67,93].

In this study, results indicated that the cells treatment with PL407-PL338-HA-SFN was able to reverse the reduction of IL-1β-induced type-2 collagen expression, thus maintaining the normal phenotype of SW1353 human cells (Fig. 5C) and showing chondroprotective effects. The results of this study indicate that cell treatment with PL407-PL338-HA-SFN was able to reverse the reduction of IL-1β-induced type II collagen expression, thus maintaining the normal phenotype of The metalloproteinases (MMPs) are a family of proteases that regulate the degradation and structural maintenance of cartilage extracellular matrix and are positively regulated under inflammatory conditions [71]. MMPs positive regulation occurs during cartilage erosion and, therefore, participates in the progression of OA. Collagenase MMP-13 preferentially cleaves type-2 collagen, which is involved in the structural and functional integrity of cartilage [72]. Although the expression of MMPs has not been quantified in this work, the lack of reduction of type II collagen expression evoked by PL407-PL338-HA-SFN is an important indicator that extracellular matrix degradation by MMPs is negatively regulated by this hydrogel formulation. Additionally, no significant differences were observed in NF-κB p65, COX-2 and type II collagen expressions after treatment with PL407-PL338-HA-SFN and non-encapsulated SFN, indicating that the SFN released from the hydrogel formulation was sufficient to modulate protein expression.

Additionally, it is important to note that the cells treated with other formulation components (PL and HA) did not inhibit the IL-1β effect. As demonstrated by the cell viability assays, both components were non-cytotoxic at the concentrations analyzed, thus indicating that the ineffectiveness in the evaluated model does not arise from a toxic response of the cells.

3.2.3. *Ex vivo pharmacological evaluation: articular cartilage degradation assays*

In this assay, the possible preventive effects of non-encapsulated SFN and PL407-PL338-HA-SFN were evaluated against joint cartilage degradation using an *ex vivo* model of OA induced by IL-1β cytokines and OSM. Cartilage explants were cultured for 21 days and the amounts of S-GAGs and remaining UA released into the culture medium were quantified every 7 days (Fig. 6).

The proteoglycans are a group of macromolecules characterized by the covalent attachment of one or more sulfated glycosaminoglycan (GAG) chains to a protein core, and are an important constituent of the extracellular matrix. GAGs, in turn, are linear, non-branched polysaccharides, made up of repeating disaccharide units, in which one of the sugar residues is an uronic acid (iduronic or glucuronic) and the other is an *N*-acetyl-glucosamine or *N*-acetyl-galactosamine [73,74]. The main known GAGs are: chondroitin sulfate, dermatan sulfate, heparan sulfate and kerat sulfate, in addition to heparin and hyaluronic acid (HA). HA is the only GAG free from sulphation and not found in the proteoglycan form [10]. Sulphated GAGs have negative charges, which increases the ability of such compounds to form complexes with various components of the ECM due to its anionic character, facilitating the interaction with many molecules of the ECM and the cell surface [73]. The S-GAGs are also involved in the binding of cations and water tissues

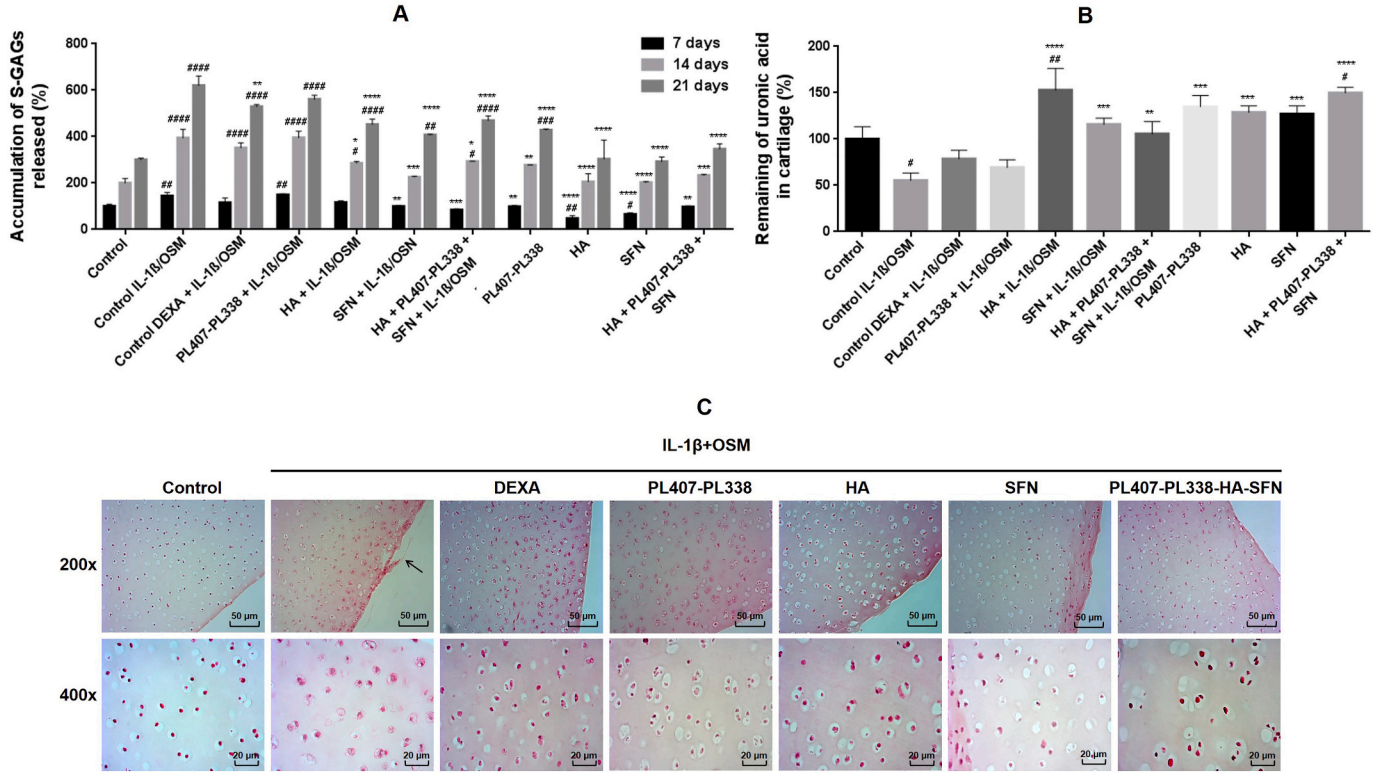

Fig. 6. Effects of PL407-PL338-HA-SFN formulation evaluated by *ex vivo* articular cartilage degradation model induced by cytokines IL-1β (20 ng/mL) and oncostatin M (OSM, 25 ng/mL). (A) Cumulative percentage of sulfated glycosaminoglycans (S-GAGs) released in the culture media during 7, 14 and 21 days. (B) Percentage of remaining uronic acid (UA) in the cartilage after 21 days. (C) Tissue morphological evaluation under H&E staining for cartilage explants after 21 days. The onset of the cartilage degradation process is evidenced with IL-1β/OSM treatment (Positive control), indicated by the arrow in an area of rough surface with fissuring. Surface roughness fibrillation and fissuring was observed in all treatments, although zonal architecture was maintained, and focal necrotic cells were observed. Values are expressed as mean ± standard deviation from three independent experiments in triplicate and analyzed by one-way ANOVA followed by Tukey-Kramer post-test. #$p < 0.05$ *vs.* the control group; ##$p < 0.01$ *vs.* the control group; ###$p < 0.001$ *vs.* the control group; *$p < 0.05$ *vs.* IL-1β/OSM group; **$p < 0.01$ *vs.* IL-1β/OSM group; ***$p < 0.001$ *vs.* IL-1β/OSM group.

retention, playing a fundamental role in the hydration of the ECM and in the regulation of molecular movements through it [75]. Depletion of S-GAGs leads to malfunction of the ECM and leads to cartilage dysfunction. The loss of GAGs is believed to be the first step in the process of cartilage degeneration [76].

The treatment with cytokines IL-1β (20 ng/mL) and OSM (25 ng/mL) evoked a significant increase in release of S-GAGs (Fig. 6A) and decreased the remaining UA percentages (Fig. 6B), when compared to the control ($p < 0.001$).

The treatment with IL-1β and OSM has shown additive effects in *ex vivo* cartilage degradation models [5,26,27], in agreement with our results. OSM has been described in inflammatory processes of the joint in patients with osteoarthritis and rheumatoid arthritis [28,29,77] and it is also known to modulate MEC degradation by controlling the balance between MMPs and the tissue inhibitors of metalloproteinases (TIMPs) at the site of damage [78]. In addition, it is an enhancer of IL-1β, TNF-α and interleukin-17 (IL-17) in the progression of cartilage destruction, promoting the production of degradation enzymes [28,29,79], which is an essential cellular mechanism for mimetizing this pathological condition using *in vitro* models, as used here.

The treatment of cartilage explants with isolated SFN and SFN in the PL407-PL338-HA-SFN formulation were both able to inhibit the IL-1β and OSM cytokine effects, thus promoting a significant ($p < 0.001$) decrease in the percentages of S-GAGs released (Fig. 6A). This result was observed from the first 7 days of exposure to the treatments, resulting in an increase in the remaining UA percentage values at the end of the 21 days of treatment (Fig. 6B).

As expected, in the presence of PL407-PL338, the percentage of S-GAGs and UA were no different from those observed after treatment with cytokines. After treatment with HA, there was a decrease in the percentage of proteoglycans released and an increase in the remaining UA in the explant cultures after 21 days. This result was considered positive, since one reason for the choice of this naturally occurring polymer arises precisely from its biocompatible and protective properties.

In fact, CD44-mediated HA effects have shown to contribute to the potential chondroprotection, proteoglycan/glycosaminoglycan synthesis and anti-inflammatory properties, important interventions for controlling the OA progression [13,25,80]. In addition, several studies have shown that the intra-articular administration of HA can restore the viscosity of the synovial fluid, protect against cartilage erosion and reduce the synovial inflammation [13,14]. However, other studies indicated that the need for multiple intra-articular injections, due to the short duration of those HA therapeutic effects, has been associated with pain, low patient compliance or possible infections due to the frequent injections [9,15,81]. Those limitations support, once again, the development of modified release systems for intra-articular administrations of incorporated drugs as an effective strategy for OA treatment.

In order to compare the formulations effects with a therapeutic control, dexamethasone (DEXA) was selected for this study. This glucocorticoid presents an anti-inflammatory action and is being administered both orally and intra-articular injections in the treatment of OA [82,83]. A significant decrease in the percentages of S-GAGs released only after 21 days of treatment with DEXA was observed. However, there was no significant increase on remaining UA percentages. It is worthy of mention that treatment with PL407-PL338-HA-SFN formulation was able to achieve protective effects on cytokine induced cartilage explants at 7 days, whereas DEXA showed effects only after 21 days.

The cartilage explant treatments with PL407-PL338-HA-SFN and its isolated components were also performed in the absence of cytokines. In general, the percentages of released S-GAGs and remaining UA in the samples were similar to the control group (untreated), demonstrating their ineffectiveness in the absence of cytokines IL-1β and OSM.

At 21 days of treatment, cartilage explants were processed by ultrafine sections (5 μm) and HE staining for analysis of possible histological changes (Fig. 6C).

The cartilage tissue presents different histological characteristics when observed from superficial to deeper zones. These differences are related to the amount and organization of extracellular matrix ECM components and chondrocyte distribution in the cartilage zones. The superficial layer shows flattened chondrocytes with fusiform shape. In the central, intermediate layer, the chondrocytes are spherical and are arranged in elongated and irregular rows, being able to form groups of cells. These chondrocyte clusters have a common origin and are therefore called isogenic groups. The histological analyses showed retraction of the chondrocytes and the matrix, allowing the observation of gaps in which the isogenic groups are found; a characteristic not observed *in vivo*. Larger cells with radial columns perpendicular to the cartilage surface are found in the deep layer [84,85].

For the control group, cartilage morphological aspects were preserved, which include a smooth surface, and intact and spheroid chondrocytes in the lacuna (the space between the cell and pericellular matrix), characteristic of the intermediate layer. On the other hand, explants treatment with IL-1β/OSM cytokines lead to changes in cartilage structure, with the presence of debris and cells with degenerative features, characterized by an alteration in the chondrocyte morphological stain when compared to normal control cells. It is also possible to detect signs of alteration in the superficial zone of the cartilage, evidenced by its rough aspect and regions of surface fissuring and fibrillation, although the cartilage zonal architecture was maintained. For the control group treated with DEXA, the morphology of the chondrocytes and tissue appearance showed similar characteristics to those observed in untreated controls and cytokines (Fig. 6C).

Cartilage explants treatment with PL407-PL338 showed no inhibition of the cytokine-induced degradative effects, since the chondrocytes showed signs of alterations, such as a rough surface and focal necrotic cells, whereas a greater irregularity was observed on the cartilage surface in the presence of HA, without morphological changes on the chondrocytes. This result is in accordance with the data obtained by quantitative analysis of released S-GAGs and remaining UA, since the treatment with PL407-PL338 did not inhibit the IL-1β/OSM effects. However, 14 days after treatment of the explants with PL407-PL338-HA-SFN, protective effects of cartilage degradation were observed (Fig. 6A and B). As previously described, chondrocytes are responsible for homeostasis of the cartilaginous tissue [86]. In this way, the presence of damaged chondrocytes directly results in alterations of the ECM structural organization and composition, since they are essential for the production and maintenance of its components.

Finally, cartilage explants treated with isolated SFN or SFN incorporated into PL407-PL338-HA showed preservation in both chondrocyte morphology and tissue surface. The cartilage degradation process begins with the roughness of the articular surface and is characterized by the decomposition of the two main macromolecular components of the ECM, the fibrillar network composed of type II collagen and proteoglycan aggregates [87,88]. In this study, evaluation of the pharmacological effects evoked by PL407-PL338-HA-SFN, in *in vitro* and *ex vivo* OA models, resulted in an increased expression of type II collagen and inhibition of the proteoglycan depletion, demonstrating the effects of the formulations for the treatment and prevention of articular degeneration.

Another important point is that the chondroprotective effects evoked by PL407-PL338-HA-SFN were significantly different ($p < 0.001$) than those observed for non-encapsulated SFN, indicating that the drug concentration released from hydrogels was sufficient to promote these effects. In this sense, according to the results of SFN release assays from PL407-PL338-HA-SFN, we estimate that total SFN release should occur in approximately 21 days, considering the drug release profiles. Thus, based on the promising *in vitro* and *ex vivo* results, it is possible to predict that a single IA injection with the PL407-PL338-HA-SFN formulation could delay the progression of OA and alleviate inflammatory symptoms for a sustained period of time. However, it is known that to confirm these

previous results, *in vivo* assays is required.

4. Final considerations

Our study reported the design, characterization, production, and *in vitro/ex vivo* pharmacological evaluation of a new approach that associated thermoreversible and biocompatible properties, looking forward SFN release, a phytochemical with promising anti-inflammatory properties for OA treatment.

In special, the incorporation of both SFN and HA into binary PL-based systems induced changes on hydrogels supramolecular structure, which means that formulations were selected associating essential features for the best predicted pharmacological performance. Since their cubic phase organization was able to modulate SFN release and drug loading percentage. In fact, the cubic phase organization is characterized by hydrophilic clusters assembled as interpenetrating channels, possibly formed by PL-based mixed micelles surrounded by an HA hydrophilic matrix network, with SFN amphiphilic molecules dispersed into both the micellar and network phases, which allowed the modulation of the drug release profile, by both diffusion and relaxation of the polymer chain processes. Finally, results reported here suggested that the new approach based on PL407-PL338-HA-SFN formulation evoked long-term *in vitro/ex vivo* chondroprotective effects, making it possible to reduce the progression of OA and alleviate inflammatory symptoms.

Funding sources

The São Paulo Research Foundation - FAPESP (Grant 2014/14457-5, 2015/14763-1, 2019/20303-4), National Council for Scientific and Technological Development - CNPq (Grant 402838/2016-5, 309207/2016-9, 307718/2019-0).

CRediT authorship contribution statement

MHMN performed the conception, *in vitro* and *ex vivo* experiments and wrote the manuscript. CBL and DRA contributed to the design, data analysis, review and wrote the manuscript. FNA, HW-N and DCF performed cell culture assays. FY, MKKDF and BK performed physicochemical analysis by SAXS. SMQ and CA-S were responsible for cell culture and western blot analysis. MN-S and MAC performed histological analysis.

Declaration of competing interest

Nothing to declare.

Acknowledgments

This research was supported by The São Paulo Research Foundation - FAPESP (Grant 2014/14457-5, 2015/14763-1, 2019/20303-4), National Council for Scientific and Technological Development - CNPq (Grant 402838/2016-5, 309207/2016-9, 307718/2019-0) and UFABC Multiuser Central Facilities (CEM-UFABC).

Appendix A. Supplementary data

In vitro release profiles evaluation, cell viability assays and *in vitro* osteoarthritis model; sulfated glycosaminoglycans (S-GAGs) and uronic acid (UA) quantification. Supplementary data to this article can be found online at doi:https://doi.org/10.1016/j.msec.2021.112345.

References

[1] P.K. Sharma, M.J. Reilly, S.K. Bhatia, N. Sakhitab, J.D. Archambult, S.R. Bhatia, Effect of pharmaceuticals on thermoreversible gelation of PEO–PPO–PEO copolymers, Colloids Surf. B Biointerfaces 63 (2008) 229–235.
[2] D. Blalock, A. Miller, M. Tilley, J. Wang, Joint instability and osteoarthritis, Clin. Med. Insights Arthritis Musculoskelet Disord. 19 (2015) 15–23.
[3] M.C. Choi, J. Jo, J. Park, H.K. Kang, Y. Park, NF-κB signaling pathways in osteoarthritic cartilage destruction, Cells. 8 (2019) 734.
[4] E. Heiss, C. Herhaus, K. Klimo, H. Bartsch, C. Gerhauser, Nuclear factor kappa B is a molecular target for sulforaphane-mediated anti-inflammatory mechanisms, J. Biol. Chem. 276 (2001) 32008–32015.
[5] F.R.K. Davidson, O. Jupp, R. de Ferrars, C.D. Kay, K.L. Culley, R. Norton, C. Driscoll, T.L. Vincent, S.T. Donell, Y. Bao, I.M. Clark, Sulforaphane represses matrix-degrading proteases and protects cartilage from destruction in vitro and in vivo, Arthritis Rheum. 65 (2013) 3130–3140.
[6] H.W. Fan, G.Y. Liu, C.F. Zhao, X.F. Li, X.Y. Yang, Differential expression of COX 2 in osteoarthritis and rheumatoid arthritis, Genet. Mol. Res. 14 (2015) 12872–12879.
[7] H. Jeong, S. Yu, J. Jung, S. Kim, Sulforaphane inhibits proliferation by causing cell cycle arrest at the G_2/M phase in rabbit articular chondrocytes, Mol. Med. Rep. 6 (2012) 1199–1203.
[8] N. Butoescu, O. Jordan, E. Doelker, Intra-articular drug delivery systems for the treatment of rheumatic diseases: a review of the factors influencing their performance, Eur. J. Pharm. Biopharm. 73 (2009) 205–218.
[9] J.Y. Ko, Y.J. Choi, G.J. Jeong, G.I. Im, Sulforaphane-PLGA microspheres for the intra-articular treatment of osteoarthritis, Biomaterials 34 (2013) 359–368.
[10] H.G. Garg, C.A. Hales, Chemistry and Biology of Hyaluronan, 1th ed., Elsevier Ltd., Oxford, Chapter 1, 2004.
[11] G. Kogan, L. Soltés, R. Stern, Hyaluronic acid: a natural biopolymer with a broad range of biomedical and industrial applications, Biotechnol. Lett. 29 (2007) 17–25.
[12] A. Mero, M. Campisi, Hyaluronic acid bioconjugates for the delivery of bioactive molecules, Polymers 6 (2014) 346–369.
[13] A. Gomis, A. Miralles, R.F. Schmidt, C. Belmonte, Intra-articular injections of hyaluronan solutions of different elastoviscosity reduce nociceptive nerve activity in a model of osteoarthritic knee joint of the Guinea pig, Osteoarthr. Cartil./OARS, Osteoarthr. Res. Soc. 17 (2009) 798–804.
[14] L.W. Moreland, Intra-articular hyaluronan (hyaluronic acid) and hylans for the treatment of osteoarthritis: mechanisms of action, Arthritis Res. Ther. 5 (2003) 54–67.
[15] K.D. Brandt, G.N. Smith Jr., L.S. Simon, Intraarticular injection of hyaluronan as treatment for knee osteoarthritis: what is the evidence? Arthritis Rheum. 43 (2000) 1192–1203.
[16] Kang, M. L.; Im, GI. Drug delivery systems for intra-articular treatment of osteoarthritis. Expert Opin. Drug Deliv. 2014, 11, 296-282.
[17] F. Artzner, S. Geiger, A. Olivier, C. Allais, S. Finet, F. Agnely, Langmuir 23 (2007) 5085–5092.
[18] M.J.M. Klaver, M.G. Buckingham, G.F. Rich, Lidocaine attenuates cytokine-induced cell injury in endothelial and vascular smooth muscle cells, Anesth. Analg. 97 (2003) 465–470.
[19] G. Dumortier, J.L. Grossiord, F. Agnely, J.C. Chaumeil, A review of poloxamer 407 pharmaceutical and pharmacological characteristics, Pharm. Res. 23 (2006) 2709–2728.
[20] L. Mayol, M. Biondi, F. Quaglia, S. Fusco, A. Borzacchiello, L. Ambrosio, M.I. La Rotonda, Injectable thermally responsive mucoadhesive gel for sustained protein delivery, Biomacromolecules 12 (2011) 28–33.
[21] L. Mayol, F. Quaglia, Borzacchiello, Assunta, L. Ambrosio, M.I. La Rotonda, A novel poloxamers/hyaluronic acid in situ forming hydrogel for drug delivery: rheological, mucoadhesive and in vitro release properties, Eur. J. Pharm. Biopharm. 70 (2008) 199–206.
[22] K.Y. Cho, T.W. Chung, B.C. Kim, M.K. Kim, J.H. Lee, W.R. Wee, C.S. Cho, Release of ciprofloxacin from poloxamer-graft-hyaluronic acid hydrogels in vitro, Int. J. Pharm. 260 (2003) 83–91.
[23] M.H.N. Nascimento, M.K. Franco, F. Yokaichiya, E. de Paula, C.B. Lombello, D. R. De Araujo, Hyaluronic acid in Pluronic F-127/F-108 hydrogels for postoperative pain in arthroplasties: influence on L properties and structural requirements for sustained drug-release, Int. J. Biol. Macromol. 1 (2018) 1–12.
[24] E.S. Figueirêdo, A.C. Macedo, P.F.R. Figueirêdo, F.S. Figueirêdo, Aplicações oftalmológicas do ácido hialurônico, Arq. Bras. Oftalmol. 73 (2010) 92–95.
[25] T. Conrozier, A. Walliser-Lohse, P. Richette, Intra articular injections of Hylan GF-20 reduce type 2 collagen degradation in patients with knee osteoarthritis: the biovisco study, Ann. Rheum. Dis. 69 (2010) 281.
[26] T.E. Cawston, A.J. Ellis, G. Humm, E. Lean, D. Ward, V. Curry, Interleukin-1 and oncostatin M in combination promote the release of collagen fragments from bovine nasal cartilage in culture, Biochem. Biophys. Res. Commun. 215 (1995) 377–385.
[27] M. Khansai, M. Boonmaleerat, P. Pothacharoen, T. Phitak, P. Kongtawelert, Ex vivo model exhibits protective effects of sesamin against destruction of cartilage induced with a combination of tumor necrosis factor-alpha and oncostatin M, BMC Complement. Altern. Med. 16 (2016) 1–12.
[28] E.M. Moran, et al., Human rheumatoid arthritis tissue production of IL-17A drives matrix and cartilage degradation: synergy with tumour necrosis factor-alpha, Oncostatin M and response to biologic therapies, Arthritis Res. Ther. v. 11 (2009) 113.
[29] E.M. Moran, R. Mullan, J. McCormick, M. Connolly, O. Sullivan, O. FitzGerald, B. Bresnihan, D.J. Veale, U. Fearon, Human rheumatoid arthritis tissue production of IL-17A drives matrix and cartilage degradation: synergy with tumour necrosis factor-alpha, oncostatin M and response to biologic therapies, Arthritis Res. Ther. 11 (2009) 113.

[30] I.R. Schmolka, Preparation and properties of pluronic F-127 gels for treatment of burns, J. Biomed. Mater. Res. 6 (1972) 571–582.
[31] M.R.C. Marques, R. Loebenberg, M. Almukainzi, Simulated biological fluids with possible application in dissolution testing, U.S. Pharmacopeia (2011) 15–28.
[32] M. Gebauer, J. Saas, F. Sohler, J. Haag, S. Söder, M. Pieper, E. Bartnik, J. Beninga, R. Zimmer, T. Aigner, Comparison of the chondrosarcoma cell line SW1353 with primary human adult articular chondrocytes with regard to their gene expression profile and reactivity to IL-1β, Osteoarthr. Cartil. 13 (2005) 697–708.
[33] C. Liu, Y. Zhang, B. Dai, Y. Ma, Q. Zhang, Y. Wang, H. Yang, Chlorogenic acid prevents inflammatory responses in IL 1β stimulated human SW 1353 chondrocytes, a model for osteoarthritis, Mol. Med. Rep. 16 (2017) 1369–1375.
[34] International Standards Organization. ISO 10993-5. 2009, p.34.
[35] Vincenti, M. P.; Brinckerhoff, C. E. Early response genes induced in chondrocytes stimulated with the inflammatory cytokine interleukin 1beta. Arthritis Res. 2001, 3,381 388.
[36] P. Alexandridis, J.F. Holzwarthf, T.A. Hatton, Micellization of poly(ethy1ene oxide)-poly(propy1ene oxide)-poly(ethy1ene oxide) triblock copolymers in aqueous solutions: thermodynamics of copolymer association, Macromolecules 27 (1994) 2414–2425.
[37] Oshiro, A.; Da Silva, D. C.; De Mello, J. C., De Moraes, V. W. R.; Cavalcanti, L. P.; Franco, M. K. K. D.; Alkschbirs, M. I.; Fraceto, L. F., Yokaichiya, F.; Rodrigues, T.; 2014.
[38] Y. Zhang, Y.M. Lam, W.S. Tan, Poly(ethylene oxide)-poly(propylene oxide)-poly (ethylene oxide)-g-poly(vinylpyrrolidone): association behavior in aqueous solution and interaction with anionic surfactants, J. Colloid Interface Sci. 285 (2005) 74–79.
[39] Y. Zhang, Molecular mechanism of rapid cellular accumulation of anticarcinogenic isothiocyanates, Carcinogenesis 22 (2001) 425–431.
[40] K. Edsman, J. Carlfors, R. Petersson, Rheological evaluation of poloxamer as an in situ gel for ophthalmic use, Eur. J. Pharm. Sci. 6 (1998) 105.
[41] G.G. Pereira, F.A. Dimer, S.S. Guterres, C.P. Kechinski, J.E. Granada, N.S. M. Cardozo, Formulation and characterization of poloxamer 407: thermoreversible gel containing polymeric microparticles and hyaluronic acid, Quim Nova 36 (2013) 1121–1125.
[42] A. Sosnik, D. Cohn, Reverse thermo-responsive poly (ethylene oxide) and poly (propylene oxide) multiblock copolymers, Biomaterials 26 (2005) 349–357.
[43] A.C.S. Akkari, J.Z.B. Papini, K.G. Garcia, M.K.K.D. Franco, L.P. Cavalcanti, A. Gasperini, M.I. Alkschbirs, F. Yokaichyia, E. de Paula, G.R. Tófoli, D.R. de Araújo, Poloxamer 407/188 binary thermosensitive hydrogels as delivery systems for infiltrative local anesthesia: Physico-chemical characterization and pharmacological evaluation, Mater. Sci. Eng. 68 (2016) 299–307.
[44] M.K.K.D. Franco, A.F. Sepulveda, A.A. Vigato, A. Oshiro, I.P. Machado, B. Kent, D. Clemens, F. Yokaichiya, D.R. de Araujo, Supramolecular structure of temperature-dependent polymeric hydrogels modulated by drug incorporation, ChemistrySelect 5 (2020) 12853–12861.
[45] M.N. Freitas, M. Farah, R.E.S. Bretas, E. Ricci-Júnior, J.M. Marchetti, Rheological characterization of Poloxamer 407 nimesulide gels, Rev. Ciênc. Farm. Básica Apl. 27 (2006) 113–118.
[46] E.J. Ricci, M.V. Bentley, M. Farah, R.E. Bretas, J.M. Marchetti, Rheological characterization of Poloxamer 407 lidocaine hydrochloride gels, Eur. J. Pharm. Sci. 17 (2002) 161–167.
[47] S.C.V. Kulkarni, A. Yaghmur, M. Steinhart, M. Kriechbaum, M. Rappolt, Effects of high pressure on internally self-assembled lipid nanoparticles: a synchrotron small-angle X-ray scattering (SAXS), Langmuir 15 (2016) 11907–11917.
[48] R. Mezzenga, J.M. Seddon, C.J. Drummond, B.J. Boyd, G.E. Schröder-Turk, L. Sagalowicz, Nature-inspired design and application of Lipidic Lyotropic liquid crystals, Adv. Mater. (2019) 31.
[49] W.K. Fong, T.L. Hanley, B. Thierry, A. Hawley, B.J. Boyd, C.B. Landersdorfer, External manipulation of nanostructure in photoresponsive lipid depot matrix to control and predict drug release in vivo, J. Control. Release 28 (2016) 67–73.
[50] L. Ambrosio, A.P.A. Borzacchiello, L. Netti, L. Nicolais, Properties of new materials: rheological study on hyaluronic acid and its derivative solutions, J. Macromol. Sci., Part A: Pure Appl. Chem. 36 (1999) 991–1000.
[51] J.W. Fahey, A.T. Zalcmann, P. Talalay, The chemical diversity and distribution of glucosinolates and isothiocyanates among plants, Phytochemistry 56 (2001) 5–51.
[52] L. Ye, Y. Zhang, Total intracellular accumulation levels of dietary isothiocyanates determine their activity in elevation of celullar glutathione and induction of phase 2 detoxification enzymes, Carcinogenesis 22 (2001) 1987–1992.
[53] A.M. Goes, S. Carvalho, R.L. Oréfice, L. Avérous, T.A. Custódio, J.G. Pimenta, M. B. Souza, M.C. Branciforti, R.E.S. Bretas, Viabilidade celular de nanofibras de polímeros biodegradáveis e seus nanocompósitos com argila montmorilonita, Polímeros 22 (2012) 34–40.
[54] M. Ifrah, S. Stienlauf, M. Shoresh, E.A. Katz, Tetrazolium-based colorimetric assay for titration of neutralizing antibodies against vaccinia virus, Immunology 11 (1998) 49–54.
[55] R.R. Miller, C.A. Macdevitt, A quantitative microwell assay for chondrocyte cell adhesion, Anal. Biochem. 192 (1991) 380–383.
[56] G. Fotakis, J.A. Timbrell, In vitro cytotoxicity assays: comparison of LDH, neutral red, MTT and protein assay in hepatoma cell lines following exposure to cadmium chloride, Toxicol. Lett. 160 (2006) 171–177.
[57] G. Repetto, A. Del Peso, J.L. Zurita, Neutral red uptake assay for the estimation of cell viability/cytotoxicity, Nat. Protoc. 3 (2008) 1115–1131.
[58] N. Tani, S. Kinoshita, Y. Okamoto, M. Kotani, H. Itagaki, N. Murakami, Interlaboratory validation of in vitro eye irritation test for cosmetic ingredients. Evaluation of cytotoxicity test on SIRC cells, Toxicol. In Vitro 13 (1999) 175–187.
[59] H.Y. Hsieh, W.Y. Lin, A.L. Lee, Y.C. Li, Y.J. Chen, K. Chen, T.H. Young, Hyaluronic acid on the urokinase sustained release with a hydrogel system composed of poloxamer 407: HA/P407 hydrogel system for drug delivery, PLoS One (2020) 15.
[60] E. Lippens, I. Swennen, J. Gironès, H. Declercq, G. Vertenten, L. Vlaminck, F. Gasthuys, E. Schacht, R. Cornelissen, Cell survival and proliferation after encapsulation in a chemically modified Pluronic((R)) F127 hydrogel, J. Biomater. Appl. 27 (2013) 828–839.
[61] J.A. Mengshol, M.P. Vincenti, C.E. Brinckerhoff, IL-1 induces collagenase-3 (MMP-13) promoter activity instably transfected chondrocytic cells: requirement for Runx-2 and activation by p38 MAPK and JNK pathways, Nucleic Acids Res. 29 (2001) 4361–4372.
[62] Y. Pei, A. Harvey, X.P. Yu, S. Chandrasekhar, K. Thirunavukkarasu, Differential regulation of cytokineinduced MMP-1 and MMP-13 expression by p38 kinase inhibitors in human chondrosarcoma cells: potential role of Runx2 in mediating p38 effects, Osteoarthr. Cartil. 14 (2006) 749–758.
[63] C. Boileau, J.P. Pelletier, G. Tardif, H. Fhmi, S. Laufer, M. Lavigne, J. Martel-Pelletier, The regulation of human MMP-13 by licofelone, an inhibitor of cyclo-oxygenases and 5-lipoxygenase, in human osteoarthritic chondrocytes is mediated by the inhibition of the p38 MAP kinase signalling pathway, Ann. Rheum. Dis. 64 (2005) 891–898.
[64] A. Liacini, J. Sylvester, W.Q. LI, M. Zafarullah, Mithramycin downregulates proinflammatory cytokineinduced matrix metalloproteinase gene expression in articular chondrocytes, Arthritis Res. Ther. 7 (2005) 777–783.
[65] H.A. Kim, Y. Yeo, H.A. Jung, Y.O. Jung, S.J. Park, S. Kim, Phase 2 enzyme inducer sulphoraphane blocks prostaglandin and nitric oxide synthesis in human articular chondrocytes and inhibits cartilage matrix degradation, Rheumatology 51 (2012) 1006–1016.
[66] C. Xu, G. Shen, C. Chen, C. Gelinas, A.N. Kong, Suppression of NF-κB and NF-κB regulated gene expression by sulforaphane and PEITC through IκBα, IKK pathway in human prostate cancer PC-3 cells, Oncogene 24 (2005) 4486–4495.
[67] M.B. Goldring, J. Birkhead, L.J. Sandell, T. Kimura, S.M. Krane, Interleukin 1 suppresses expression of cartilage-specific types II and IX collagens and increases types I and III collagens in human chondrocytes, J. Clin. Invest. 82 (1988) 2026–2037.
[68] A.W. Palmer, C.G. Wilson, E.J.M.S. Baum, M.E. Levenston, Composition-function relationships during IL-1-induced cartilage degradation and recovery, Osteoarthr. Cartil. 17 (2009) 1029–1039.
[69] J.A. Tyler, H.P. Benton, Synthesis of type II collagen is decreased in cartilage cultured with interleukin 1 while the rate of intracellular degradation remains unchanged, Coll. Relat. Res. 8 (1988) 393–405.
[70] I. Yaron, F.A. Meyer, J.M. Dayer, I. Bleiberg, M. Yaron, Some recombinant human cytokines stimulate glycosaminoglycan synthesis in human synovial fibroblast cultures and inhibit it in human articular cartilage cultures, ArthritisRheum. 32 (1989) 173–180.
[71] Hu, P.; Chen, W.; Bao, J.; Jiang, L.; Wu, L. Cordycepin modulates inflammatory and catabolic gene expression in interleukin 1beta induced human chondrocytes from advanced stage osteoarthritis: an in vitro study. Int. J. Clin. Exp. Pathol. 2014, 7, 6575 6584.
[72] Y.Z. Chen, W. Zhang, Y.K. Huang, F. Gao, X.L. Fang, Dual-functionalc(RGDyK)-decorated Pluronic micelles designed for antiangiogenesis and thetreatment of drug-resistant tumor, Int. J. Nanomedicine 10 (2015) 4863–4881.
[73] R.S. Souza, Pinhal, M.A. Da Silva, Interactions in physiological processes: the importance of the dynamics between extracellular matrix and proteoglycans, Arquivos Brasileiros de Ciências da Saúde 36 (2011) 48–54.
[74] A.D. Theocharis, S.S. Skandalis, G.N. Tzanakakis, N.K. Karamanos, Proteoglycans in health and disease: novel roles for proteoglycans in malignancy and their pharmacological targeting FEBSJ 277 (2010) 3904–3923.
[75] E. Ruoslahti, Proteoglycans in cell regulation, J. Biol. Chem. 264 (1989) 13369–13372.
[76] J.Y. Wang, M.H. Roehrl, Glycosaminoglycans are a potential cause of rheumatoid arthritis, Proc. Natl. Acad. Sci. 99 (2002) 14362–14367.
[77] W. Hui, M. Bell, G. Carroll, Detection of oncostatin M in synovial fluid from patients with rheumatoid arthritis, Ann. Rheum. Dis. 56 (1997) 184–187.
[78] U. Fearon, R. Mullan, T. Markham, M. Connolly, S. Sullivan, A.R. Poole, O. FitzGerald, B. Bresnihan, D.J. Veale, Oncostatin M induces angiogenesis and cartilage degradation in rheumatoid arthritis synovial tissue and human cartilage cocultures, Arthritis Rheum. 54 (2006) 3152–3162.
[79] W. Hui, A.D. Rowan, C.D. Richards, T.E. Cawston, Oncostatin M in combination with tumor necrosis factor alpha induces cartilage damage and matrix metalloproteinase expression in vitro and in vivo, Arthritis Rheum. 48 (2003) 3404–3418.
[80] R.D. Altman, A. Manjoo, A. Fierlinger, F. Niazi, M. Nicholls, The mechanism of action for hyaluronic acid treatment in the osteoarthritic knee: a systematic review, BMC Musculoskelet. Disord. 16 (2015) 321–331.
[81] S.S. Leopold, W.J. Warme, P.D. Pettis, S. Shott, Increased frequency of acute local reaction to intra-articular hylan GF-20 (synvisc) in patients receiving more than one course of treatment, J. Bone Joint Surg. 84 (2002) 1619–1623.
[82] A. Abou-Raya, S. Abou-Raya, T. Khadrawi, M. Helmii, Effect of low-dose oral prednisolone on symptoms and systemic inflammation in older adults with moderate to severe knee osteoarthritis: a randomized placebo-controlled trial, J. Rheumatol. 41 (2014) 53–59.
[83] T. Bjørnland, A.A. Gjærum, A. Møystad, Osteoarthritis of the temporomandibular joint: an evaluation of the effects and complications of corticosteroid injection compared with injection with sodium hyaluronate, J. Oral Rehabil. 34 (2007) 583–589.

[84] J. Angel, P. Razzano, D. Grande, Defining the challenge: the basic science of articular cartilage repair and response injury, Sports Med. Arthrosc. Rev. 11 (2003) 168–181.
[85] S.A.J. Fox, A. Bedi, S.A. Rodeo, The basic science of articular cartilage: structure, composition, and function, Sports Health 1 (2009) 461–468.
[86] T. Aigner, S. Soeder, J. Haag, IL-1 and BMPS – interactive players of cartilage matrix degradation and regeneration, Eur. Cell. Mater. 12 (2006) 49–56.
[87] R. Brocklehurst, M.T. Bayliss, A. Maroudas, H.L. Coysh, M.A. Freeman, P. A. Revell, S.Y. Ali, The composition of normal and osteoarthritic articular cartilage from human knee joints. With special reference to unicompartmental replacement and osteotomy of the knee, J. Bone Joint Surg. Am. 66 (1984) 95–106.
[88] S. Grenier, M.M. Bhargava, P.A. Torzilli, An in vitro model for the pathological degradation of articular cartilage in osteoarthritis Stephanie, J. Biomech. 47 (2014) 645–652.
[89] D.R. De Araujo, Pluronics f-127/l-81 binary hydrogels as drug-delivery systems: influence of physicochemical aspects on release kinetics and cytotoxicity, Langmuir 30 (2014) 13689–136698.
[90] de Araujo, D. R.; Oshiro, A.; Silva, D. C.; Akkari, A. C. S.; Mello, J. C.; Rodrigues, T. Poloxamers as drug-delivery systems: Physicochemical, pharmaceutical and toxicological aspects. In: Durán N; Guterres, S. S.; Alvez, O. L. (Org.). Nanotoxicology: Materials, Methodologies and Assessments. 1 ed. New York: Springer, 2014, p. 281–298.
[91] Z.H. Liu, D.H. Liu, L.L. Wang, J.A. Zhang, N. Zhang, Docetaxel-loaded pluronicP123 polymeric micelles: in vitro and in vivo evaluation, Int. J. Mol. Sci. 12 (2011) 1684–1696.
[92] Mariano, K. C. F.; Nascimento, M. H. M.; Querobino, S. M.; Campos, E. V. R.; Oliveira, J. L.; Yokaichiya, F.; Franco, M.K.K.D.; Alberto-Silva, C.; De Paula, E.; Lombello, C. B.; Lima, R.; Fraceto, L. F.; De Araujo, D. R. Influence of chitosan-tripolyphosphate nanoparticles on thermosensitive polymeric hydrogels: structural organization, drug release mechanisms and cytotoxicity. Int. J. Polym. Mater. Polym. Biomater., 2020, 69, 592–603, 2020.
[93] Z.H. Zheng, X.Y. Li, J. Ding, J.F. Jia, P. Zhu, Allogeneic mesenchymal stem cell and mesenchymal stem cell-differentiated chondrocyte suppress the responses of type II collagenreactive T cells in rheumatoid arthritis, Rheumatology 47 (2008) 22–30.
[94] H.A. Kim, Y. Yeo, W. Kim, S. Kim, Phase 2 enzyme inducer sulphoraphane blocks matrix metalloproteinase production in articular chondrocytes, Rheumatology 48 (2009) 932–938.
[95] C. Chung, J. Mesa, M.A. Randolph, M. Yaremchuk, J.A. Burdick, Influence of gel properties on neocartilage formation by auricular chondrocytes photoencapsulated in hyaluronic acid networks, J. Biomed. Mat. Res. A 77 (2006) 518–525.
[96] M. Gebauer, J. Saas, F. Sohler, J. Haag, S. Söder, M. Pieper, E. Bartnik, J. Beninga, R. Zimmer, T. Aigner, Comparison of the chondrosarcoma cell line SW1353 with primary human adult articular chondrocytes with regard to their gene expression profile and reactivity to IL-1β, Osteoarthritis Cartilage 13 (2005) 697–708.
[97] L. Zeng, W. Wang, X.F. Rong, Y. Zhong, P. Jia, G.Q. Zhou, R.H. Li, Chondroprotective effects and multi-target mechanisms of Icariin in IL-1 beta-induced human SW 1353 chondrosarcoma cells and a rat osteoarthritis model, Int. Immunopharmacol. 18 (2014) 175–181.
[98] M. Salim, W.F.N.W. Iskandar, M. Patrick, N. Idayu, Zalid, R. Hashim, Swelling of bicontinuous cubic phases in guerbet glycolipid: effects of additives, Langmuir 32 (2016) 5552–5561.
[99] H.A. Kim, Y. Yeo, W. Kim, S. Kim, Phase 2 enzyme inducer sulphoraphane blocks matrix metalloproteinase production in articular chondrocytes, Rheumatology 48 (2009) 932–938.
[100] M.A. Pattoli, J.F. MacMaster, K.R. Gregor, J.R. Burke, Collagen and aggrecan degradation is blocked in interleukin-1-treated cartilage explants by an inhibitor of IκB kinase through suppression of metalloproteinase expression, J. Pharmacol. Exp. Ther. 315 (2005) 382–388.